REPORT DOCUMENTATION PAGE

Form Approved
OMB No. 0704-0188

PLEASE DO NOT RETURN YOUR FORM TO THE ABOVE ORGANIZATION.

1. REPORT DATE *(DD-MM-YYYY)*	2. REPORT TYPE	3. DATES COVERED *(From - To)*
07-30-2012	Journal Article	

4. TITLE AND SUBTITLE

Water Mass Bio-optical Properties in the Monterey Bay Region: Fluorescence-based Inference of Shifts in Phytoplankton Photophysiology

5a. CONTRACT NUMBER

5b. GRANT NUMBER

5c. PROGRAM ELEMENT NUMBER
0602435N

6. AUTHOR(S)
J.K. Jolliff, R.W. Gould, B. Penta, W.J. Teague, S. DeRada, F.P. Chavez and R.A. Arnone

5d. PROJECT NUMBER

5e. TASK NUMBER

5f. WORK UNIT NUMBER
73-6463-01-5

7. PERFORMING ORGANIZATION NAME(S) AND ADDRESS(ES)
Naval Research Laboratory
Oceanography Division
Stennis Space Center, MS 39529-5004

8. PERFORMING ORGANIZATION REPORT NUMBER
NRL/JA/7330--12-0795

9. SPONSORING/MONITORING AGENCY NAME(S) AND ADDRESS(ES)
Office of Naval Research
One Liberty Center
875 North Randolph Street, Suite 1425
Arlington, VA 22203-1995

10. SPONSOR/MONITOR'S ACRONYM(S)
ONR

11. SPONSOR/MONITOR'S REPORT NUMBER(S)

12. DISTRIBUTION/AVAILABILITY STATEMENT
Approved for public release, distribution is unlimited.

13. SUPPLEMENTARY NOTES
20120802043

14. ABSTRACT

A physical and bio-optical field survey of the Monterey Bay area was conducted during May -June 2008. The combined bio-optical and physical data may be summarized as a transition between two end-member states during the late spring to summer upwelling season: (1) the mesotrophic, nanoflagellate-dominated, low-salinity surface waters (chlorophyll-a ~ 0.5 -2 mg m^{-3}; S < 33.4) of the California Current and (2) the eutrophic, diatomaceous, higher salinity surface waters (chlorophyll-a > 2 mg m^{-3}; S > 33.8) of Monterey Bay and adjacent continental shelf areas. High-resolution and collocated spectrophotometric, fluorometric and CTD data obtained from a towed platform indicated low-salinity subarctic-origin surface waters intruded into Monterey Bay on 4 June. The dark in vivo fluorometry (IVF) phytoplankton response normalized to particle absorption at 676 nm (the apparent fluorescence efficiency, AFE) was nearly fourfold larger in this water mass type compared to higher salinity surface waters more typical of Monterey Bay. The collocated fluorescence and optical data were then used to estimate in situ irradiance values and determine apparent light saturation intensities (I'_k) based on the remarkably consistent AFE water column inflection points. I'_k values retrieved from the low-salinity surface waters were approximately half those obtained over the continental shelf. An analysis of concomitant HPLC data, in addition to historical data for the region, suggest these observed fluorescence trends may be indicative of taxon-specific variation in photophysiology.

15. SUBJECT TERMS
Monterey Bay,diatoms,ocean optics,water masses

16. SECURITY CLASSIFICATION OF:			17. LIMITATION OF ABSTRACT	18. NUMBER OF PAGES	19a. NAME OF RESPONSIBLE PERSON
a. REPORT	b. ABSTRACT	c. THIS PAGE			Jason K. Jolliff
Unclassified	Unclassified	Unclassified	UU	16	19b. TELEPHONE NUMBER *(Include area code)* 228-688-5308

Water mass bio-optical properties in the Monterey Bay region: Fluorescence-based inference of shifts in phytoplankton photophysiology

J. K. Jolliff,[1] R. W. Gould Jr.,[1] B. Penta,[1] W. J. Teague,[1] S. DeRada,[1] F. P. Chavez,[2] and R. A. Arnone[1]

Received 2 September 2011; revised 16 April 2012; accepted 6 June 2012; published 26 July 2012.

[1] A physical and bio-optical field survey of the Monterey Bay area was conducted during May–June 2008. The combined bio-optical and physical data may be summarized as a transition between two end-member states during the late spring to summer upwelling season: (1) the mesotrophic, nanoflagellate-dominated, low-salinity surface waters (chlorophyll-$a \sim 0.5$–2 mg m^{-3}; S < 33.4) of the California Current and (2) the eutrophic, diatomaceous, higher salinity surface waters (chlorophyll-$a > 2$ mg m^{-3}; S > 33.8) of Monterey Bay and adjacent continental shelf areas. High-resolution and collocated spectrophotometric, fluorometric and CTD data obtained from a towed platform indicated low-salinity subarctic-origin surface waters intruded into Monterey Bay on 4 June. The dark in vivo fluorometry (IVF) phytoplankton response normalized to particle absorption at 676 nm (the apparent fluorescence efficiency, AFE) was nearly fourfold larger in this water mass type compared to higher salinity surface waters more typical of Monterey Bay. The collocated fluorescence and optical data were then used to estimate in situ irradiance values and determine apparent light saturation intensities (I'_k) based on the remarkably consistent AFE water column inflection points. I'_k values retrieved from the low-salinity surface waters were approximately half those obtained over the continental shelf. An analysis of concomitant HPLC data, in addition to historical data for the region, suggest these observed fluorescence trends may be indicative of taxon-specific variation in photophysiology. Specifically, the subarctic water mass-associated pelagic nanoflagellate group likely possesses a fundamentally different photosynthetic architecture than large diatoms prototypical of coastal upwelling regimes.

Citation: Jolliff, J. K., R. W. Gould Jr., B. Penta, W. J. Teague, S. DeRada, F. P. Chavez, and R. A. Arnone (2012), Water mass bio-optical properties in the Monterey Bay region: Fluorescence-based inference of shifts in phytoplankton photophysiology, *J. Geophys. Res.*, *117*, C07019, doi:10.1029/2011JC007568.

1. Introduction

[2] The goal of the Naval Research Laboratory's (NRL) Bio-Optical Studies of Predictability and Assimilation for the Coastal Environment (BIOSPACE) program is to forecast bio-optical and physical properties of the coastal zone on the timescale of atmospheric model forecasts (~1–5 days) using coupled ecosystem-hydrodynamic numerical simulations. This goal requires an extensive interdisciplinary field effort to constrain/validate modeling activities, as well as improve our understanding of biological-physical interactions. Accordingly, the first BIOSPACE field observation campaign was conducted during 2008 in the Monterey Bay region (Figure 1). Following the template of the previous Autonomous Ocean Sampling Network (AOSN) experiments in Monterey Bay [*Ramp et al.*, 2009], the BIOSPACE field program sought a comprehensive collection of in situ data from the deployment of autonomous platforms, moorings, and ship station sampling while leveraging available remote sensing information and high-frequency Doppler radar stations.

[3] Here we present a synthesis of this field effort, with specific emphasis upon relating biological and bio-optical properties with physical properties of specific water mass types. The concept of biological properties specific to plankton being consistently delineated by independently described physical water masses was demonstrated by *Fager and McGowan* [1963] and more recently applied to biological studies of Monterey Bay [*Osborn et al.*, 2007]. Here we show that this is a useful context for the descriptive analysis of

[1]Ocean Sciences Branch, Naval Research Laboratory, Stennis Space Center, Mississippi, USA.
[2]Monterey Bay Aquarium Research Institute, Moss Landing, California, USA.

Corresponding author: J. K. Jolliff, Ocean Sciences Branch, Naval Research Laboratory, Stennis Space Center, MS 39529, USA. (jason.jolliff@nrlssc.navy.mil)

0148-0227/12/2011JC007568

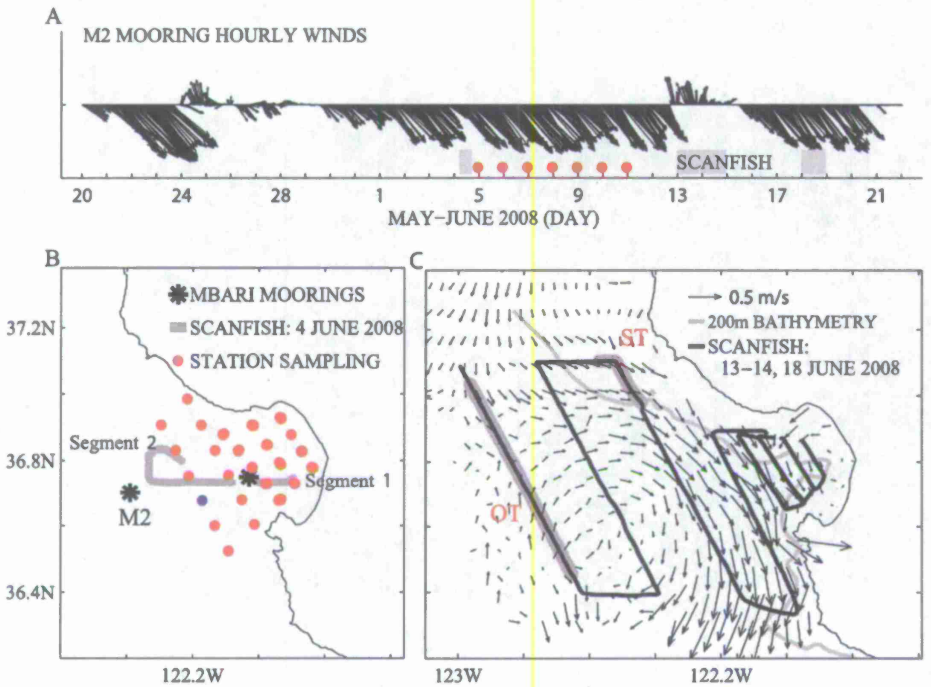

Figure 1. (a) Time line of the BIOSPACE ScanFish (SF) deployments (gray) and ship station sampling (red dots) with MBARI moorings M2 wind vectors. (b) Map of the SF and station sampling deployments in the MB area. SF surveys on 4 June are shown in gray for segments 1 and 2. The remaining SF tracks are in black. The station sampling for the extraction of bottle chlorophylls, nutrients, and HPLC data are shown in red, with a single station where observed salinity was less than 33.3 shown in blue. (c) High-frequency Doppler radar estimates of surface currents in the MB region, 25-h means ending 4 June, 0:00 GMT are overlaid on the SF tracks (data available at http://www.cocmp.org/).

our field data. Moreover, an understanding of the coupled physical and bio-optical features observed provides a criterion for ecosystem-hydrodynamic model evaluation that moves beyond univariate model and data comparison statistics [*Jolliff et al.*, 2009; *Stow et al.*, 2009].

[4] As is typical of contemporary ocean observational campaigns, the BIOSPACE field study included the deployment of multiple conventional chlorophyll-*a* fluorometers on a wide range of platforms (Slocum electric gliders, towed vehicles, moorings, autonomous underwater vehicles, CTD rosettes, horizontal profiling optics packages, underway ship flow-through systems). The 2008 field survey alone obtained on the order of $\sim 10^6$ fluorometer observations. Ostensibly, these millions in vivo fluorescence (IVF) datum may serve as a collective proxy for the space/time distribution of phytoplankton chlorophyll-*a* concentration [*Lorenzen*, 1966]. However, the IVF data collected appear to be no better than an order-of-magnitude accurate indicator of phytoplankton pigment concentration. Whereas these data may be useful for descriptive analysis of the presence or absence of phytoplankton blooms, more quantitative treatment of these data is not tractable. This failing of conventional fluorometry data to serve as a reliable proxy for phytoplankton pigment concentration has long been recognized [*Alpine and Cloern*, 1985; *Cullen*, 1982; *Falkowski and Kolber*, 1995; *Loftus and Seliger*, 1975; *Strickland*, 1968].

[5] Nevertheless, fluorescence is a specific physiological response of the photosynthetic apparatus; effectively a pathway of activated chlorophyll deexcitation in competition with the photochemical pathway and energy dissipation as heat [*Krause and Weis*, 1991]. An alternative usage of IVF data is to place the observed fluorescence intensity response in the context of the overall physiological energy transformation within photosystem II (PSII) of the phytoplankton photosynthetic apparatus [see *Huot and Babin*, 2010]. Fluorescence properties observed in situ are thus indicative of photophysiological properties of natural phytoplankton populations [*Falkowski and Kolber*, 1995; *Kiefer and Reynolds*, 1992]. The challenge presented by these IVF data is to carefully make inferences about such photophysiological properties via analysis of the additional bio-optical and environmental variables observed [*Cullen*, 1982; *Kiefer*, 1973; *Sackmann et al.*, 2008]. Herein IVF data are examined where concomitant spectral absorption, scattering, and backscattering coefficients were observed as well as the physical properties of seawater. Independent estimates of phytoplankton pigment concentration, particle absorption, and light attenuation provided an appropriate context to make inferences from these IVF data that may improve understanding of integrated biological-physical processes in this region.

2. Methods

2.1. Study Site

[6] The Monterey Bay (hereinafter MB) region is part of the California Current System (CCS), and it is located within

an extended regional transition zone between the subarctic Pacific and the North Pacific subtropical gyre [*Roden*, 1991]. The subarctic front, approximately the 33.8 isohaline [*Tully and Barber*, 1960], lies along ~40–43°N latitude and curves southward west of 150°W to form the western boundary of the CCS [*Lynn*, 1986]. Thus, water mass characteristics of the transition zone are influenced by the different temperature and salinity (T/S) properties of the subarctic and the subtropics. In the MB region, apparent T/S signatures of both water mass types may be found [*Warn-Varnas*, 2007]. The relative predominance of these contrasting water mass characteristics at any given time and location is brought about by a complex interplay between the meandering and shoreward translation of the equatorward flowing California Current [*Checkley and Barth*, 2009], the prevailing mode of the wind stress (upwelling/downwelling-favorable) [*Storlazzi et al.*, 2003], mesoscale eddies and their interaction with both the California Current and upwelling jets [*Paduan and Rosenfeld*, 1996], and the seasonally recurring surface expression of poleward flows along the California coast [*Chelton et al.*, 1988].

[7] Herein an attempt is made to relate these physical water mass characteristics to bio-optical signatures. The pelagic/low-salinity subarctic Pacific is regarded as an iron-limited system [*Boyd et al.*, 2004], and in contrast to similar latitudes in the North Atlantic, there is no distinct spring bloom. Subarctic Pacific surface chlorophyll-*a* concentration (hereinafter chl) values there are consistently on the order of ~0.5–2 mg m^{-3} [*Miller et al.*, 1991]. Upwelling along the central California coast, however, results in surface chl values an order of magnitude higher [*Collins et al.*, 2003]. Within MB (an open embayment spanning approximately 40 km north-to-south), a highly diverse and variable phytoplankton assemblage is observed [*Rines et al.*, 2010] and chl values range to >500 mg m^{-3} [*Lee et al.*, 2007; *Ryan et al.*, 2009].

[8] With respect to temperature and salinity, California Current water tends to be cold and fresh due to a subarctic origin, whereas MB surface waters and surface waters of more southerly origin are warmer and more saline, reflecting near-equatorial sources [*Breaker and Broenkow*, 1994]. Accordingly, Spiciness (Π) is a useful state variable for this analysis [*Flament*, 2002]. Π isopleths are approximately orthogonal to those of density in T/S space [*Fofonoff*, 1985] such that on an isopycnal surface some water masses may be "spicier" (warmer/saltier) than others. This analysis is largely restricted to the upper ~80 m during a seasonal period of upwelling favorable wind stress along the coast (Figure 1a); diapyncal mixing of subarctic-origin California Current surface waters with recently upwelled, higher salinity waters near the coast appears to generally follow constant Π isopleths. Large Π deviations from the prevailing Π isopleths were interpreted as indicative of the addition (positive-Π) or removal (negative-Π) of thermal energy due to air/sea exchange processes.

2.2. Bio-Optical Survey and Analysis Methods

[9] As part of NRL's BIOSPACE project, an extensive field campaign was conducted in the MB area from 30 May to 19 June 2008 based primarily on board the *R/V Point Sur* (Moss Landing Marine Laboratories). Observations included ship station CTD casts (Figure 1) with multiple analyses performed on water samples from the Niskin bottle rosette. Macronutrient and chlorophyll assays were performed using methods detailed in *Pennington and Chavez* [2000]. High Performance Liquid-Chromatography (HPLC) analyses were performed on near-surface water samples filtered through GF/F filters, stored in liquid nitrogen and shipped to the Horn Point Laboratory (University of Maryland) for analysis following standard NASA HPLC protocols [*Hooker et al.*, 2005]. Aliquots of GF/F-filtered and liquid nitrogen-stored sample water were also obtained for spectrophotometric determination of absorption coefficients (Analytical Spectral Devices FieldSpec spectroradiometer with a spectral range of ~338 nm–~1069 nm at ~1.4 nm resolution). Total absorption coefficients were partitioned into phytoplankton, particulate detritus, and dissolved contributions following methods described in *Mitchell et al.* [2000].

[10] This analysis focuses primarily on the observations from the ScanFish MK II (SF) platform (Figure 1). The SF is a remotely operated and towed vehicle that was piloted in the water column from just below the surface to about 80 m depth. A multiple sensor suite was mounted on the SF platform: AC-9 spectrophotometer for the measurement of multispectral absorption and scattering coefficients; WET Labs Environmental Characterization Optics (ECO)-BB3 instrument used here for the retrieval of particle backscattering coefficients, Sea-Bird Electronics CTD, and a WET Labs ECO chlorophyll-*a* fluorometer. Here we isolate 2170 quasi-vertical profiles from both the descent and ascent of the towed platform, with a mean spatial resolution of ~2 observations per vertical meter. The AC-9 raw data were corrected for temperature, salinity, and scattering effects [*Gould et al.*, 1999; *Pegau et al.*, 1997; *Zaneveld et al.*, 1994].

[11] The chlorophyll fluorescence sensor was factory calibrated to yield apparent "chlorophyll" values using a linear operator and these data were not corrected for additional quenching effects [*Cullen*, 2008; *Sackmann et al.*, 2008]. Instead, the fluorometer chlorophyll concentration values were reassigned as arbitrary fluorescence units (AFU), i.e., these data were interpreted as an indicator of the fluorescence intensity response without additional presumptions regarding pigment concentration or phytoplankton biomass. Similar treatment of conventional "chlorophyll-*a*" fluorometer data as "relative fluorescence units" may be found in *Ryan et al.* [2005] and *Yu et al.* [2002].

[12] Data from the SF-mounted AC-9 spectrophotometer were used as an alternative proxy for phytoplankton pigment concentration. An AC-9-based particle absorption at 676 nm (a_p-676) was calculated by subtracting the literature pure water value [*Pope and Fry*, 1997] from the total absorption coefficient observations and presuming the absorption contribution from non-living organic matter was negligible at longer wavelengths. The observed relationship between our spectrophotometric filter pad measurements of particle absorption against the bottle chl measurements provided an empirical fit that was applied to the AC-9 data set (Figure 2). The robust correspondence between log-transformed a_p-676 and bottle chl determinations ($r^2 = 0.88$, $n = 160$) was consistent with previous studies [*Babin et al.*, 2003; *Bricaud et al.*, 1995] and provided a means to transform the SF-mounted AC-9 data into a new proxy for phytoplankton pigment concentration, which is referred to hereinafter as chl-*a*p (mg m^{-3}).

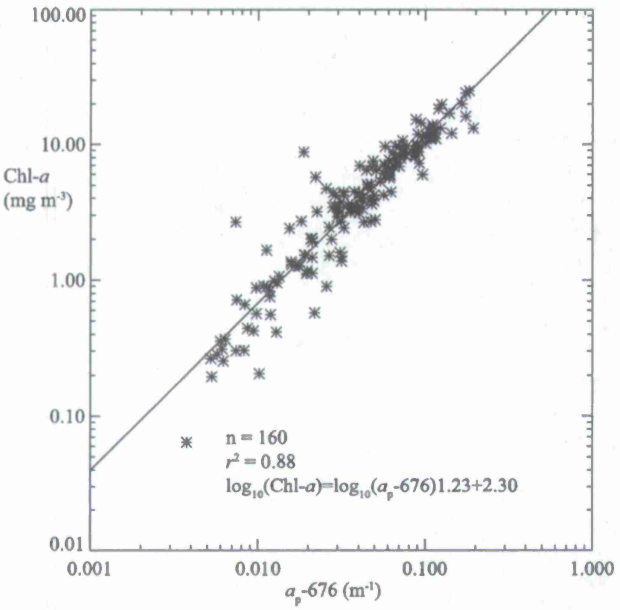

Figure 2. Bottle chlorophyll measurements from ship station sampling versus spectrophotometric determination of particle absorption coefficients (676 nm).

[13] When the AC-9-based proxies for phytoplankton pigment concentration were compared to the collocated SF fluorescence data, patterns emerged that were broadly consistent with what is known about phytoplankton fluorescence physiology. Since it is not customary to analyze conventional chlorophyll fluorometer data in this manner, some additional variables were defined to aid in the analysis. The Apparent Fluorescence Efficiency (AFE) was defined as the in vivo fluorescence response (F, Ex/Em 470/695 nm, quantified as AFU) normalized by the AC-9 chlorophyll estimate (chl-*a*p)

$$\mathrm{AFE_c} = \frac{\mathrm{F(AFU)}}{\text{chl-}ap}. \quad (1)$$

The subscript "c" indicates that the AFE value is determined from the chlorophyll estimate based on the AC-9 absorption value. Similarly, the AFE values were also examined with respect to the original a_p-676 nm coefficient

$$\mathrm{AFE_p} = \frac{\mathrm{F(AFU)}}{ap\text{-}676\ \mathrm{nm}}. \quad (2)$$

[14] In both calculations the intent is to estimate the fluorescence efficiency of the phytoplankton population. The word "apparent" is used throughout to emphasize that conventional chl fluoromtery (i.e., excitation with a weak flash of light that does not significantly perturb the electron transport system of the photosynthetic units) is quite distinct from "active" or "variable" fluorometry techniques such as Fast Repetition Rate Fluorometry (FRRF) wherein repetitive or saturating flashes of light are used to fully reduce photosystem II (PSII) to obtain the maximum fluorescence response and other derivative fluorescence parameters on each individual sample [*Suggett et al.*, 2009]. Here, the analysis compensates for an incomplete fluorescence diagnostic on each datum by examining trends for a very large aggregate "weak probe" IVF data set ($\sim 2 \times 10^5$) in the context of concomitantly collected optical and physical data. Particularly useful was the estimate of the in situ irradiance field integrated over the Photosynthetically Active Radiation spectral range (400–700 nm). These irradiance estimates were calculated by combining the ship meteorological data with the SF profile Inherent Optical Property (IOP) data. Details for this procedure are provided in section A1.

[15] The ancillary "historical data" used in this analysis refers to the bimonthly California Cooperative Fisheries Investigations (CalCOFI) Line 67 station surveys conducted between 1989 and 2007 and biweekly hydrographic and biological surveys conducted near MBARI permanent mooring M1 (36°44.8′N, 122°1.3′W) [*Chavez et al.*, 2002; *Pennington and Chavez*, 2000]. These data were collected and archived by the Monterey Bay Aquarium Research Institute (MBARI) Ocean Biology Group, and post-1996 biweekly cruises were conducted as part of the Studies of Ecological and Chemical Responses to Environmental Trends (SECRET) program [*Chavez et al.*, 2002]. Further information on data retrieved from MBARI permanent moorings and previous micronutrient surveys of the MB area are provided in section A2.

3. Results

3.1. Bio-Optical Properties and Water Mass Types

[16] The SF platform tows were first conducted during 4 June along a transect beginning within MB (Segment 1; Figure 1b) and resuming outside of MB (Segment 2) during a brief pause in the prevailing northwesterly winds (Figure 1a). The potential shoreward intrusion of subarctic-origin water was indicated by SF surface salinities below 33.4 (Segment 2; Figure 3); whereas within MB the SF-detected salinities remained above 33.8 (Segment 1; Figure 3). Low temperature (~9.0°C) and comparatively high salinity (~34.0) observations made within MB (Segment 1) were likely indicative of recently upwelled North Pacific Deep Water (NPDW). Higher temperatures for salinities >33.8 (a positive-Π deviation) suggest subsequent warming of NPDW within MB. Warmer waters were coincident with higher total 440 nm absorption coefficients in both transects (Figure 3a), although MB surface water absorption coefficients were an order-of-magnitude higher.

[17] The 4 June T/S observations on Segment 2 appear to have captured atypical conditions with respect to historical observations in this area. Only 13.4% of the historical CTD values (n = 55,015) recorded in the upper 200 m meet a negative-Π criterion over the $25 < \sigma_\theta < 26$ density interval, in contrast to 60% of the Segment 2 SF observations. Coincident Mooring M2 observations confirm the presence of this negative-Π water mass in the area (Figure 4). A review of these M2 T/S data (1999–2008) revealed that the frequency of appearance for this water mass type ranged from ~1–30% of M2 observations during the May through June period of each year.

[18] This low-salinity, negative-Π water mass type appeared to be a cold halocline form of subarctic upper water (SUW) and was likely advected into the MB area via

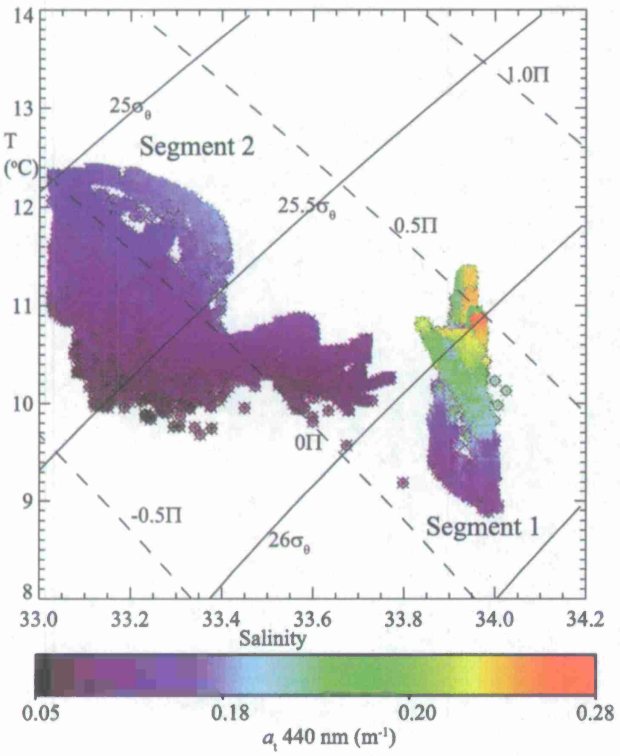

Figure 3. T/S plot of 4 June SF surveys, Segments 1 (S > 33.8) and 2 (S < 33.8). Color contours are the AC-9 total absorption coefficients (440 nm) at each point. Density and Π (dashed line) contours are overlaid in T/S space.

the meandering of the offshore California Current [*Warn-Varnas*, 2007]. Indeed, CODAR surface current estimates indicated the presence of an anticyclonic eddy centered just west of Mooring M2 at the time of the SF Segment 2 observations (Figure 1c). Negative Spiciness is interpreted here as an indication of a comparative thermal energy deficit over the observed salinity range. The sign of the Spiciness state variable is an arbitrary convention; however, it conveniently contrasts with more prototypical positive halocline Π. Previous observations of atypically negative-Π upper halocline water in the CCS have been attributed to anomalous surface cooling in the subarctic source water region followed by advection farther south [*Freeland et al.*, 2003].

[19] The remainder of the SF survey T/S properties generally fell into one of three T/S domains: (1) higher salinity MB surface water that appears to result from the mixing and warming of recently upwelled NPDW; (2) low-salinity, positive-Π surface water from the offshore transect (OT, Figure 1c); and (3) transitional T/S surface water properties between these end points. The 33.2 to 33.8 halocline waters for the remainder of the data were confined to the 0.0 to 0.5 Π isopleths (Figure 4). These data suggest that negative-Π SUW is distinct from typical CCS surface waters in this region. One may interpret the more typical warmer halocline waters as indicative of diapycnal mixing between upwelling of colder, higher salinity waters along the shelf and higher temperature waters within the coastal to California Current "transition zone" [*Collins et al.*, 2003] where isopycnal surfaces slope upwards toward the margin and the 33.4 surface salinity isopleth delineates coastal waters from the offshore California Current.

[20] This analysis of water mass physical properties suggests that the phytoplankton population of Segment 2 (negative-Π; S < 33.4) is likely indicative of a truly pelagic and subarctic character without diapycnal mixing with shoreward water masses, and by inference, coastal phytoplankton populations found there. Moreover, Segment 1 and 2 fluorescence data were recorded at night, thus sunlight-stimulated fluorescence quenching was unlikely to be a contaminant of these data. Indeed, the fluorescence signal per unit absorption from Segment 2 was over threefold higher than Segment 1 (Figure 5). Although the total absorption coefficient ranges for Segment 1 (representative of MB surface waters) ranged to much larger values, the apparent increase in AFE*p* for Segment 2 was evident even where the particle absorption values were comparable (e.g., 0.02 m^{-1} a_p 676; Figure 5a). Conversion of these *a*p-676 values to chl-*a*p revealed the same trend with respect to the fluorescence response; however, maximum Segment 2 surface chl-*a*p values were in the ~2–3 mg m^{-3} range, whereas Segment 1 surface chl-*a*p values ranged upwards to ~15 mg m^{-3}. This suggests that the AFE differences may be concomitant to a transition in trophic state between the respective water masses, i.e., mesotrophy (~2 mg m^{-3} surface chl) to eutrophy (>2 mg m^{-3} surface chl [cf. *Bricaud et al.*, 2004]).

[21] If indeed dark AFE is a distinguishable bio-optical signature of phytoplankton populations that are endemic to specific water mass types, then it would be expected that Segments 1 and 2 may serve as end points with dark AFE's at intermediate salinities ranging quasi-conservatively between them. This expected trend was observed (Figure 6). These AFE$_c$ observations for dark (<10 μE m^{-2} s^{-1} incident

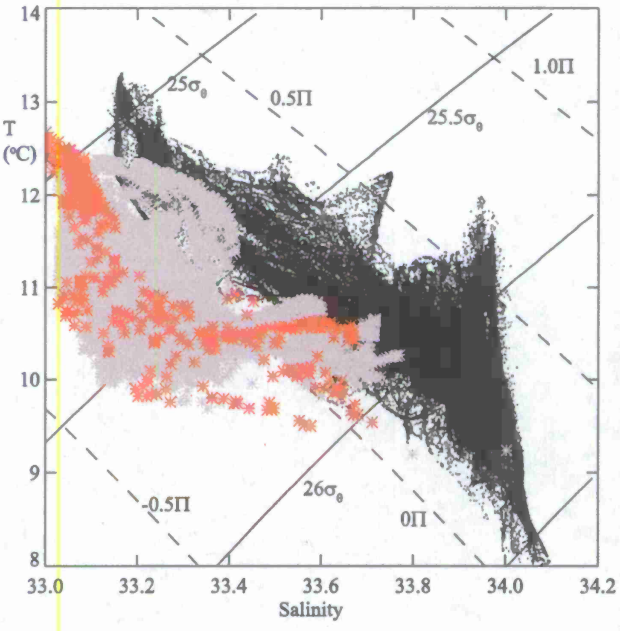

Figure 4. All SF data are shown in black with the 4 June SF Segment 2 shown in gray. The mooring M2 observations (red) confirm the negative-Π water mass presence also detected by the SF-mounted CTD.

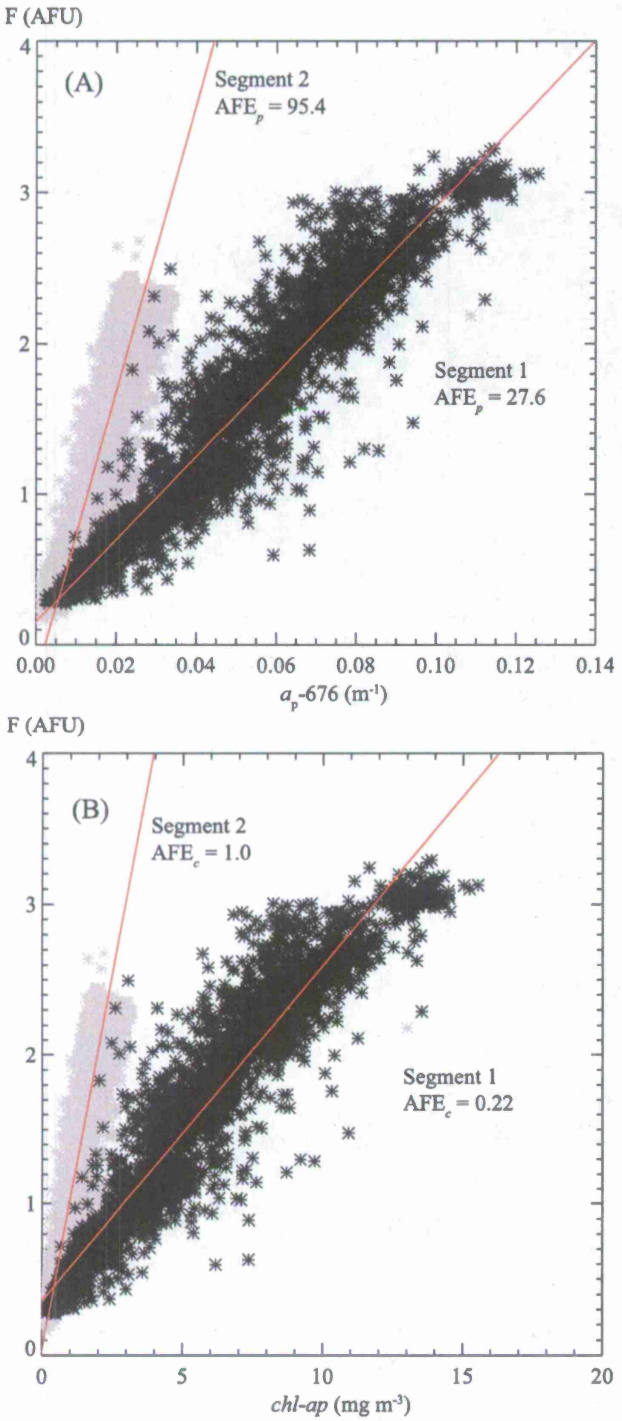

Figure 5. (a) Fluorescence (F; AFU) versus AC-9 estimated particle absorption at 676 nm for Segment 1 (black) and Segment 2 (gray): the linear regression line is shown in red and the slope is indicated as AFE_p. (b) As in Figure 5a but the chl-*a*p values are used instead and the AFE_c slope value estimates are given for the respective transects.

scalar PAR) and near-surface waters (<20 m depth) appeared to corroborate the notion that certain biological properties of plankton may be delineated by independently described physical properties of seawater [*Fager and McGowan*, 1963].

3.2. Apparent Fluorescence Quenching

[22] Exceptions to these AFE patterns occurred where near-surface fluorescence observations were made during daylight hours. For example, the fluorescence relationships to *a*p-676 for the night phase of the outer transect (OT, Figure 1c) were approximately log linear (Figure 7a). This relationship was used as an initial proxy for the expected dark fluorescence response, i.e., it was assumed that the PSII reaction centers were open (represented by the term: F*o) during this time. Quenching of fluorescence was inferred by deviation from this a_p-676 -to-F*o log linear relationship during daylight hours. The deviation from dark values was positive toward an apparent peak in fluorescence and then a significant negative deviation occurred (Figure 7b).

[23] Since fluorescence quenching was suggested by deviations from F*o, the estimate of F*o was subtracted from the observed fluorescence intensity (F; AFU) to calculate an apparent variable fluorescence (F*v)

$$F^*v = F - F^*o, \tag{3}$$

where

$$F^*o = 10^{(\log_{10}(ap\text{-}676)X+Y)} \tag{4}$$

and the log linear regression coefficients (X, Y) were determined from the nearest set of available dark fluorescence and a_p-676 observations.

[24] The F*v profiles resulting from these calculations mimicked fluorescence induction curves: F*v increased from near zero at depth to a local water column peak as PSII reaction centers were presumably closed and fluorescence efficiency increased (photochemical quenching variability; PQ, Figure 7c). Ascending higher into the water column, the inflection back toward lower F*v values was then likely due to the dominance of nonphotochemical quenching (NPQ), i.e., high-light intensities resulted in potential oxidative stress or damage.

[25] It is important to distinguish the apparent variable fluorescence (F*v) peak observed here from the fluorescence maximum as observed with variable fluorescence techniques [*Falkowski and Kolber*, 1995; *Kolber and Falkowski*, 1993]. The true florescence maximum occurs when all the primary quinone-type electron acceptors (Q_A) of PSII are fully reduced [*Krause and Weis*, 1991], and this may not have occurred in the apparent maximum of these F*v profiles. Nevertheless, it is presumed that the F*v inflection point under ambient irradiance indicates the effective saturation of PSII reaction centers; thus the F*v inflection points were interpreted as apparent irradiance saturation values (I'_k). These values for the outer transect profiles were remarkably consistent at ~67 μE m^{-2} s^{-1} (Figure 8a). The zero crossing, where the observed fluorescence was below the expected dark fluorescence, consistently occurred at ~405 μE m^{-2} s^{-1}. Speculatively, negative F*v values may have been indicative of true photoinhibitory damage to PSII reaction centers, i.e., reaction centers damaged from oxidative stress were no longer

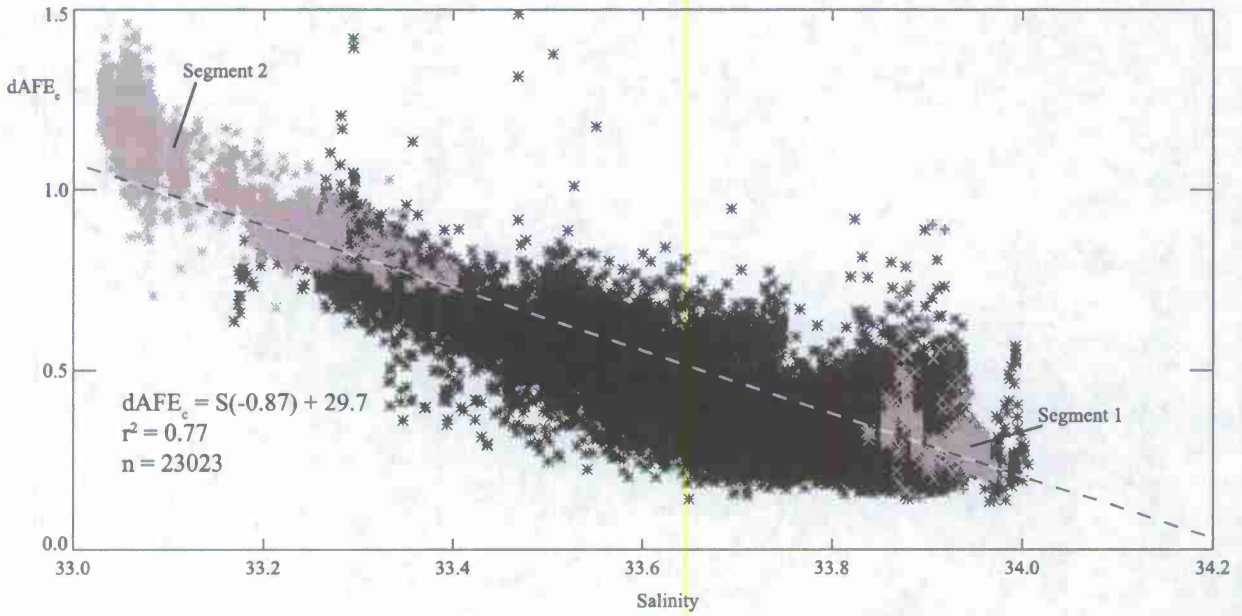

Figure 6. Estimates of Apparent Fluorescence Efficiency (AFE_c) versus salinity for all dark and near surface (<20 m) SF observations: Gray asterisks correspond to the 4 June Segment 2 observations (top left) and the Segment 1 observations (bottom right), all other observations are black. The linear regression (AFE_c versus salinity) trend line is shown (dashed line).

functional [*Maxwell and Johnson*, 2000]. This is in contrast to energy-dependent nonphotochemical quenching that involves changes in the PSII absorption cross-section and thermal dissipation of energy but is not associated with structural damage to the photosynthetic apparatus [*Kiefer and Reynolds*, 1992; *Maxwell and Johnson*, 2000]. AFE_p versus in situ irradiance patterns confirm the identical apparent irradiance saturation peak at 67 μE m^{-2} s^{-1} (Figure 8b).

[26] Whereas the fluorescence versus irradiance (*F* versus *I*) curves are not functionally identical to photosynthesis versus irradiance curves (*P* versus *I*) [*Kolber and Falkowski*, 1993; *Stegmann et al.*, 1992], the apparent F*v inflection points here are likely to occur at an in situ irradiance close to the saturation of photosynthetic activity [*Kiefer and Reynolds*, 1992]. These inferred I'_k values were low compared to literature (*P* versus *I* curve) I_k values [*Jassby and Platt*, 1976] and would be indicative of dark-acclimated microflora [*Chan*, 1978], or I_k values more typical of high-latitude phytoplankton [*Gilstad and Sakshaug*, 1990]. The genuine I_k values may be different than these estimated quantities, but it was apparent that phytoplankton endemic to low-salinity/subarctic-origin surface water mass types were consistently responding to oxidative stress at comparatively low irradiances throughout the solar period of the offshore SF transect (Figures 9a and 9b). The surface salinity was below 33.4 and surface chl was on the order of ~2 mg m^{-3} (Figure 9c), suggesting that this "offshore" transect was representative of California Current mesotrophic conditions.

[27] These F*v versus irradiance calculations were repeated for a case of apparent nonphotochemical quenching in surface waters much closer to the coast and over the continental shelf northwest of MB (ST in Figure 1c). The mean surface salinity for this transect was 34.0; mean surface chl (chl-*a*p) was 3.3 mg m^{-3} and ranged as high as 6.9 mg m^{-3}. Here again the apparent quenching patterns (as a function of the estimated in situ irradiance) were consistent. However, the collective "shelf water" patterns found here were distinct from those observed offshore. The inflection point (I'_k) was observed at irradiant intensities more than double the offshore values: ~147 μE m^{-2} s^{-1}. Further, the F*v values did not fall below zero over the same high irradiance levels (>400 μE m^{-2} s^{-1}; Figure 10a). Peak AFE_p values occurred at twice the in situ irradiance as the offshore transect, but the peak AFEp values were half as high. AFEp subsurface peaks were also detected on some SF profiles obtained within MB (data not shown) at a similar in situ irradiance value (~152 μE m^{-2} s^{-1}). This suggests there is some inherent distinction between neritic phytoplankton populations and those farther offshore that is manifest in these apparent irradiance saturation values.

3.3. Phytoplankton Species Composition and Dissolved Nutrients

[28] Bulk contrasts in the phytoplankton community fluorescence responses may be due to differences in phytoplankton community composition and associated variations in pigment content [*Alpine and Cloern*, 1985; *Beutler et al.*, 2003; *Falkowski and Kolber*, 1995] as well as nutritional status [*Behrenfeld et al.*, 2006; *Hou et al.*, 2007]. Both of these conditions, in turn, may impact light acclimation responses and associated changes in apparent fluorescence properties. Strictly taxon-specific apparent fluorescence property differences would be consistent with the notion that subarctic-origin surface water masses contain pelagic pico- and nanophytoplankon populations (<20 μm cell diameter) whereas MB waters contain neritic populations composed predominantly of diatomaceous microphytoplankton (>20 μm cell diameter)

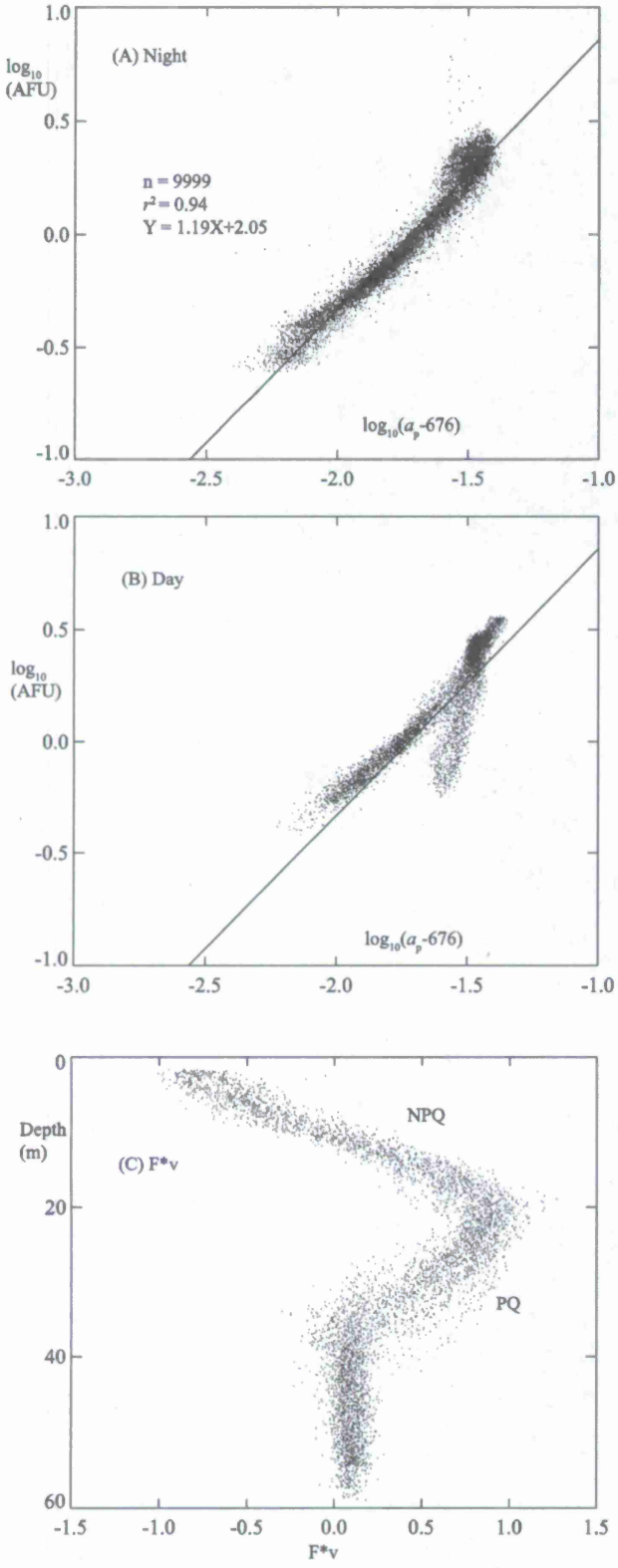

[*Chavez et al.*, 1991; *Collins et al.*, 2003; *Wilkerson et al.*, 2000].

[29] HPLC data collected during station sampling allow for an evaluation of potential fluorescence-based inferences of phytoplankton community shifts and associated differences in pigment content. The mean pigment-based microphytoplankton proportion factor [*Hooker et al.*, 2005] was 90% (n = 58) during the station survey, with one notable outlier at 30% (Table 1). This reflects a station sampling bias confined closer to the coast and the interior of MB (Figure 1b). Nonetheless, the respective outlier bottle salinity was 33.28, compared to S > 33.70 for the remaining HPLC samples. Significant departures of this outlier sample from the expected HPLC variable distributions ($p < 0.01$) occurred for a greater proportion of chlorophyll-*b* and photoprotective carotenoids (Table 1). The sample was also significantly elevated in 19′-butaloyloxyfucoxanthin, 19′-hexanoyloxyfucoxanthin, and lutein; generally indicative of greater pelagophyte, prymnesiophyte, and chlorophyte abundance, respectively [*Riegman and Kraay*, 2001]. This group is generally <20 μm cell diameter and may be referenced as the nanoflagellate group [*Jeffrey and Vesk*, 1997]. Pigment markers for this nanoflagellate group are a distinctive feature of HPLC data obtained in the subarctic North Pacific [*Fujiki et al.*, 2009].

[30] Similar trends were evidenced by alternative taxonomic identification methods in the historical data. Cell counts collected over 1989–2006 were sorted by total autotrophic biomass and the mean percentage contributions from picophytoplankton and diatoms were calculated (Figure 11a). Diatoms crossed 50% of the estimated total chl threshold at approximately ~2 mg m^{-3} chl. Thus the threshold between mesotrophic and eutrophic surface waters, established herein at ~2 mg m^{-3} total chl, was also an approximate transition point into dominance of diatomaceous flora. These percentage estimates were calculated by converting cell volume carbon estimates to chlorophyll-*a* values via a constant conversion factor of 47.2, which is the mean carbon-to-chlorophyll-*a* ratio when cell carbon estimates were compared to bottle chlorophyll-*a* assays in the historical data (Figure 11b). Collectively, these data are consistent with previous work demonstrating a general trend toward microphytoplankton dominance at eutrophic (>2 mg m^{-3}) chl values [*Bricaud et al.*, 2004; *Li*, 2002], which tend to consist of large diatoms in coastal upwelling systems [*Walsh*, 1988].

[31] In the SF data set, the low-salinity phytoplankton communities (S < 33.4) reached maximum chl-*a*p values of ~2–3 mg m^{-3}; higher chl-*a*p values corresponded to higher salinities and a shift in the IVF responses toward lower AFE's. Given the hypothesis that phytoplankton community species composition, cell size, and pigment composition

Figure 7. Log plot of fluorescence (F, AFU) versus particle absorption at 676 nm (a) during the night hours (01:52–04:51 local time) of the outer transect and (b) during daylight hours (13:21–14:43 local time). The expected "dark" fluorescence response regression line as a function of a_p-676 nm is shown in Figures 7a and 7b. (c) Daylight hour profiles of fluorescence from the outer transect (13:21–14:43 local time). The apparent variable fluorescence (F*v) calculation is described in the text. (PQ) indicates presumed photochemical quenching and (NPQ) indicates presumed nonphotochemical quenching.

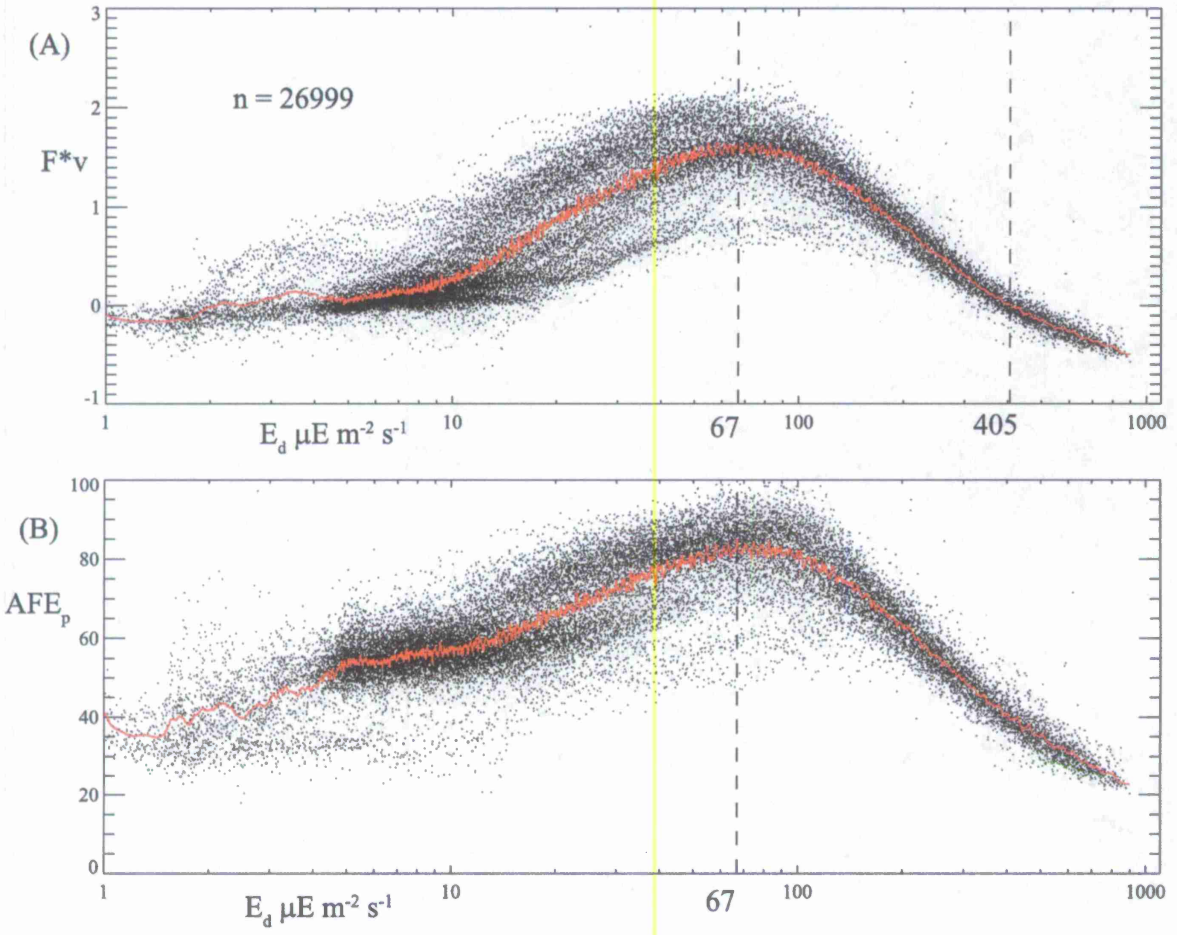

Figure 8. (a) Apparent variable fluorescence (F*v) versus irradiance for the outer SF transect survey. The trend line (red) is the smoothed data, dashed lines indicate the inflection point and zero crossing of the trend line. (b) The AFEp for the same set of points; the dashed line indicates the inflection point for the smoothed data.

generally trend in broadly consistent ways as a function of the total autotrophic biomass in this system, nutrient concentrations were also examined as an additional constraint on the transition from pelagic mesotrophy to coastal eutrophy. As observed elsewhere [*Kamykowski et al.*, 2002], nitrate versus temperature plots for the upper ocean (<200 m) conformed to a linear trend in our data as well as historical data for the MB region (Figure 12). The nitrate versus temperature zero ordinate intercept, the nitrate depletion temperature (NDT), was 14.2°C during the 2008 BIOSPACE survey (n = 638; r^2 = 0.89) and 14.4°C for the historical data (n = 7773; r^2 = 0.83). The mean surface temperature for the SF outer transect was 11.8°C (<20 m); the mean temperature for the Segment 2 observations was 9.3°C (<20 m). In both cases, the temperatures were well below the recent and historical NDT calculations. Although strictly concomitant nitrate observations were not obtained with the SF fluorescence and absorption data, it is probable that surface nitrate was present at detectable concentrations along both transects. Indeed, the aforementioned outlier HPLC and low-salinity (S = 33.28) Niskin bottle sample contained 10.6 µM nitrate. Other macronutrients (phosphate, silicilic acid) were detected and generally abundant with respect to nitrate at *Redfield et al.* [1963] proportions (data not shown). These observations strongly suggest that macronutrient limitation or stress is unlikely to explain the bio-optical and fluorescence trends in these data.

[32] The transition from the pelagic nanoflagellate to the neritic diatom phytoplankton communities in this transitional system may instead be influenced by varying degrees of iron limitation [*Ryan et al.*, 2005; *Bruland et al.*, 2001; *Fitzwater et al.*, 2003; *Johnson et al.*, 1999; *King and Barbeau*, 2011]. Supporting evidence for this iron hypothesis would be a corresponding trend in surface dissolved iron concentrations from low values (<1.0 nM) at lower salinities offshore to higher values (>1.0 nM) corresponding to higher salinities over the continental shelf. Indeed, this pattern was observed during the MUSE (2000) Monterey Bay field experiment (9–31 August; Figure 13). Surface dissolved iron concentrations in excess of 1 nM were observed at surface

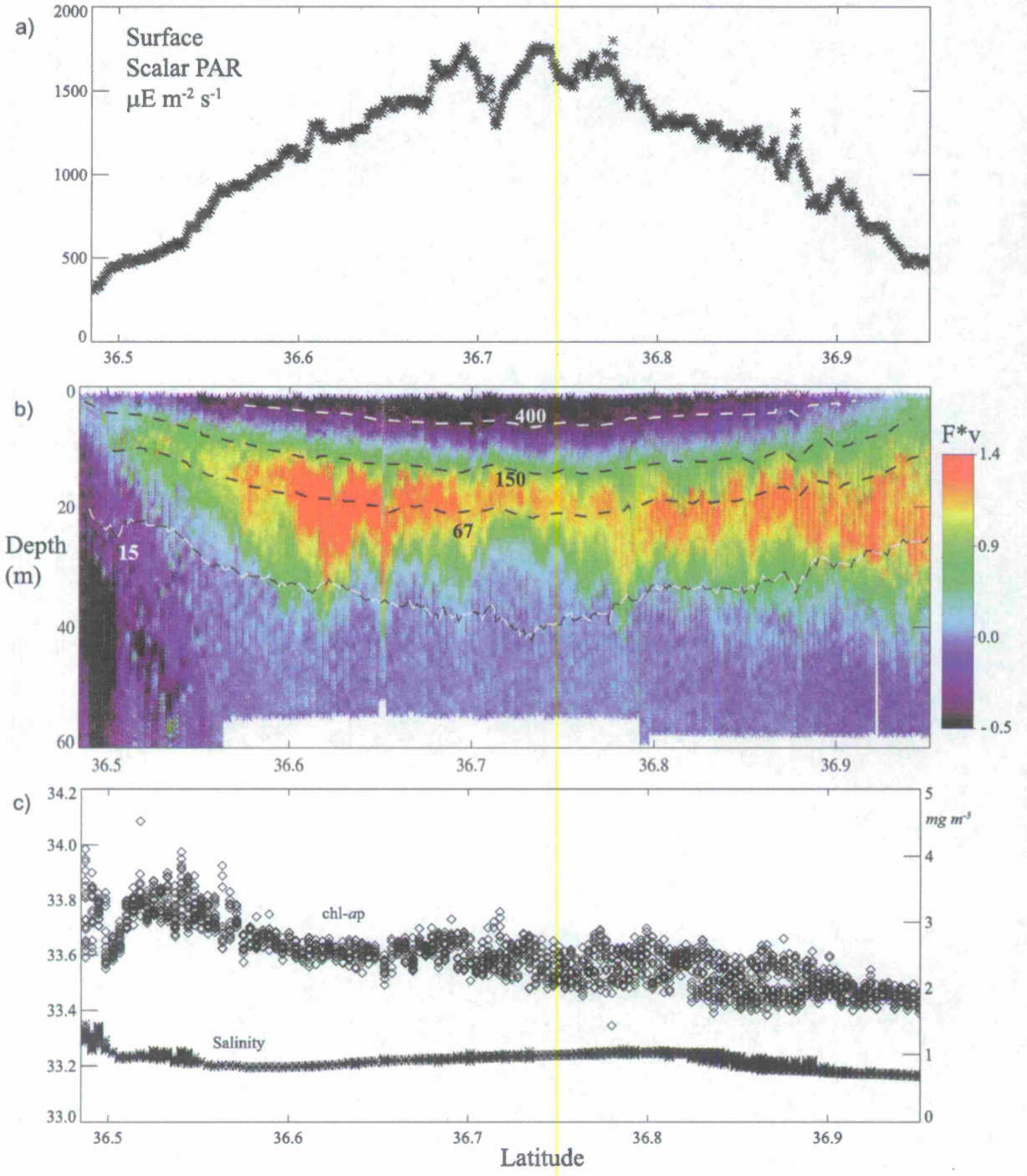

Figure 9. (a) Surface Scalar PAR as measured by the QSR 2200 sensor on board the *R/V Point Sur* during the outer transect. (b) The corresponding depth distribution of calculated apparent variable fluorescence values (F*v); estimated in situ downwelling planar PAR irradiance values are indicated for 400, 150, 67, and 15 μE m^{-2} s^{-1}. (c) The corresponding surface (<5 m) salinity and chl-*a*p observations.

salinities above 33.4, but not at salinities below this threshold value (Figure 12). Other iron data collected in this region confirm this trend [see *Johnson et al.*, 2001]. Recall that the 33.4 surface salinity isopleth has been previously used to delineate subarctic-origin surface waters of the California Current from those of the coastal transition zone [*Collins et al.*, 2003]. Culture studies of isolated phytoplankton strains from the North Pacific and suggest iron-limitation of the specific growth rate for large diatoms (>20 μm cell diameter) occurs at ambient dissolved iron concentrations below 1 nM [*Takeda*,

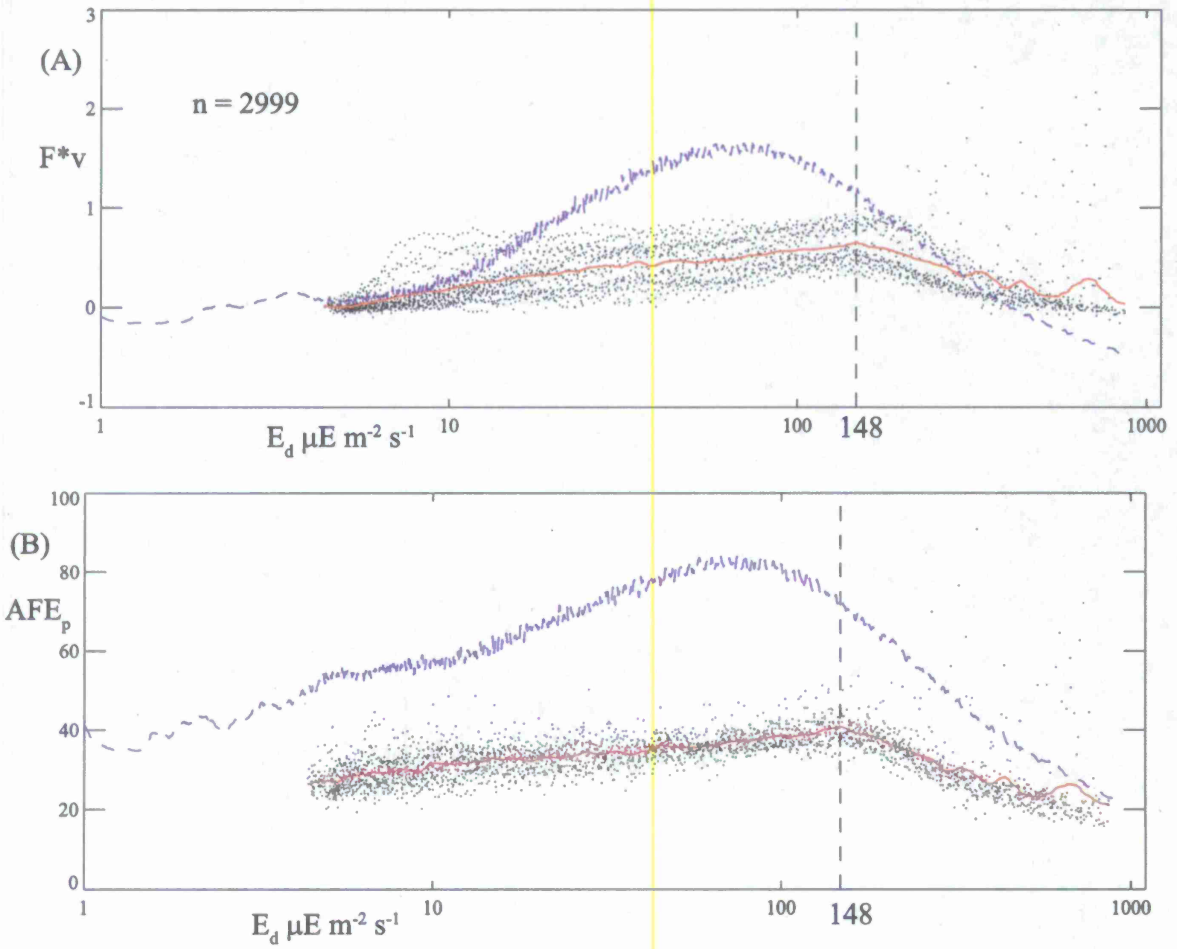

Figure 10. (a) Apparent variable fluorescence and (b) apparent fluorescence efficiency versus irradiance (as in Figure 8) for a shelf transect (ST) northwest of MB (12:00–12:53 local time; see Figure 1c). The smoothed trend line (red) inflection points are indicated by the dashed lines. The blue line is the trend from the offshore transect (OT; Figure 8), for comparison.

2011]. In contrast, pelagic phytoplankton isolates appear better adapted to low-dissolved iron conditions (<1 nM) conditions [*Takeda*, 2011; *Strzepek and Harrison*, 2004].

4. Discussion

[33] The transition from the comparatively low-dissolved iron environment of the subarctic-origin California Current to the more iron-replete upwelling waters along the California coast is attendant to a phytoplankton-species composition transition (pelagic nanoflagellates to diatomaceous microphytoplankton) that is manifest as not only a change in accessory pigment composition (Table 1) but also a probable shift in the architecture of the photosynthetic apparatus. It is this latter photophysiological shift that may explain the principal results from sections 3.1 and 3.2: a two to fourfold increase in the apparent fluorescence per unit absorption (AFE_p) or chl (AFE_c) and a simultaneous halving of the apparent irradiance saturation (I′k; Figure 10b). For example, these I′k ($\mu E\ m^{-2}\ s^{-1}$) values are directly related to other photophysiological phytoplankton variables [*Kolber and Falkowski*, 1993; *Kiefer and Reynolds*, 1992]

$$I'_k \cong I_k = \frac{1}{\sigma_{PSII}\tau_P}, \tag{5}$$

where σ_{PSII} is the effective (functional) absorption cross-section of PSII ($m^2\ \mu E^{-1}$ for unit consistency but more commonly expressed as $Å^2$ $quanta^{-1}$) and τ_P (seconds) is the minimum steady state transit time for an electron to transition from water to the terminal electron acceptor at light saturation. The effective absorption cross-section is the product of the optical absorption due to photosynthetic pigments and the probability that an exciton will be transferred to the PSII reaction center core to perform photochemical work [*Mauzerall and Greenbaum*, 1989]. Absorption cross-sections are more generally a measure of the effective target area for photons to strike the photosynthetic unit. Larger PSII "target areas" may manifest as a higher apparent yield of fluoresce per unit chl since ~95% of fluorescence per unit chl signal

Table 1. Physical and HPLC Data[a]

	Mean	Standard Deviation	Value	Z-Score
Salinity	33.92	0.10	33.28	−6.40
Density	25.96	0.15	25.29	−4.47
[But fuco]	0.010	0.011	0.074	5.81
[Hex fuco]	0.034	0.028	0.217	6.48
[Lutein]	0.003	0.002	0.016	5.42
[PPC]/[TCaro]	0.776	0.064	0.590	−2.90
[PSC]/[TCaro]	0.224	0.064	0.410	2.90
[PPC]/[TPig]	0.075	0.024	0.160	3.50
[PSC]/[TPig]	0.925	0.024	0.840	−3.50
Microphytoplankton Fraction	0.904	0.091	0.300	−6.62
Nanophytoplankton Fraction	0.057	0.064	0.490	6.81
Picophytoplankton Fraction	0.040	0.031	0.210	5.57
[TChl b]/[TChl a]	0.016	0.013	0.094	6.04
[Hex fuco]/[Fuco]	0.031	0.142	1.080	7.41

[a]The low-salinity surface sample is compared to the total sample distributions (n = 58) for HPLC variables where the S < 33.3 sample meets the $p < 0.01$ ($|z| > 2.58$) criterion. Note: 19′-butaloyloxyfucoxanthin = [But fuco]; 19′-hexanoyloxyfucoxanthin = [Hex fuco]; PPC = photoprotective carotenoids; PSC = photosynthetic carotenoids; TCaro = total carotenoids; TChl b = total chlorophyll b pigments; TChl a; total chlorophyll *a* pigments; Fuco = fucoxanthin.

emanates from PSII [*Johnson et al.*, 1997; *Kiefer and Reynolds*, 1992], whereas chl is distributed within PSII and photosystem I (PSI).

[34] Clearly a doubling of σ_{PSII} would also likely result in a halving of I'_k via equation (5). Change in σ_{PSII} by a factor of ~1.5 to 3 is within the range of natural variability for σ_{PSII} [*Suggett et al.*, 2004, 2009]. Active fluorescence techniques (FRRF) are routinely used to estimate σ_{PSII} via examination of the increase in fluorescence (F) from minimal (F_o) to maximal (F_m) under successive flashes of light. For example, *Moore et al.* [2006] found a linear correspondence between the ratio of the photosynthetic carotenoid 19′but to chlorophyll-*a* (HPLC data) and σ_{PSII} (FRRF) where surface σ_{PSII} values appeared to double following a horizontal cross-shelf gradient. Similarly, the outlier low-salinity HPLC sample in these data (Table 1) contained a 19′but: chlorophyll-*a* pigment ratio an order of magnitude above (0.072 g:g) the higher-salinity 19′but:chlorophyll-*a* average (0.003 g:g). Thus the difference in taxonomic composition implied by this particular HPLC contrast (pelagophytes) may as well be indicative of taxon-specific changes in σ_{PSII}.

[35] Further extrapolation from our HPLC data, however, is problematic since the sample was taken from the surface (<5 m depth) and contained comparatively elevated photoprotective carotenoids (Table 1). The significant decline in (negative) F*v for low-salinity surface waters observed elsewhere (Figure 8), suggests severe light stress and so photoprotective carotenoids in the light harvesting complexes for this sample may have served to enhance the thermal dissipation pathway at the expense of lowering σ_{PSII}. Conversely, the generally lower σ_{PSII} for large phytoplankton may serve as a competitive advantage in a high light and resource rich environment nearer the coast: smaller antenna complexes may be more rapidly repaired and reconstituted from damage caused by excessive irradiance [*Falkowski and Oliver*, 2007]. Indeed, shelf observations of F*v at 800 μE m^{-2} s^{-1} are approximately the same as at 10 μE m^{-2} s^{-1} (Figure 10); this is at least suggestive of a superior acclimative capacity under the conditions of supersaturating irradiance.

[36] The other term in equation (5), the photochemical electron transport rate ($1/\tau_P$), is subject to similar variations as a result of light acclimation/stress as well as macro- or micronutrient deficiencies [*Falkowski et al.*, 1992]. However, recent work has highlighted some broadly applicable taxon-specific trends in σ_{PSII} that may explain these data. *Suggett et al.* [2009] provide a comprehensive review of laboratory and field FRRF σ_{PSII} estimates; they find that large changes in σ_{PSII} are most significantly correlated to taxon-specific gradients in cell size (larger cells → smaller σ_{PSII}). This trend was largely confined to eukaryotes, but it is certainly consistent with the nanoflagellate to large diatom trend

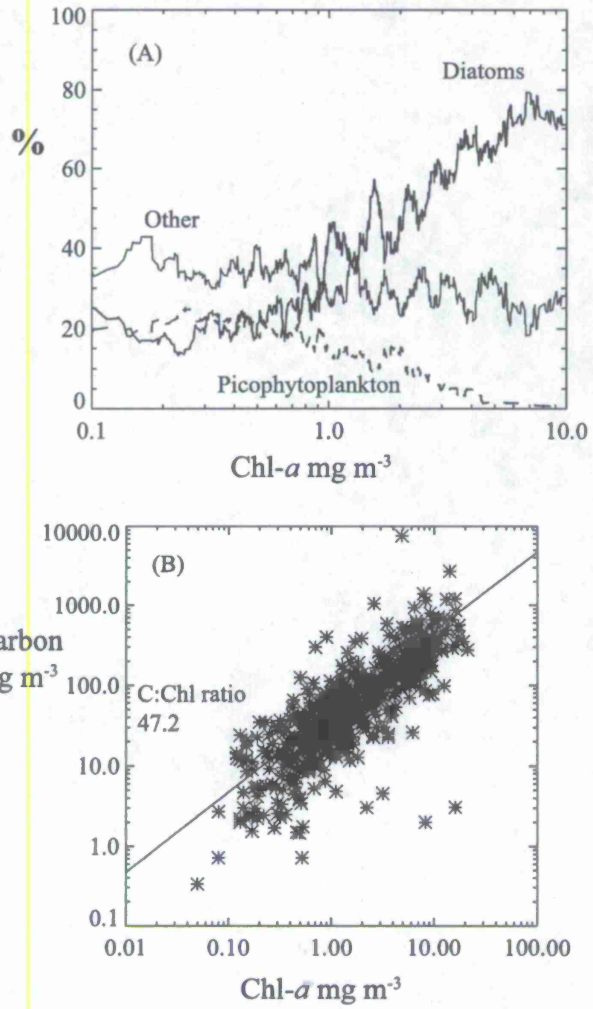

Figure 11. (a) Historical data (as referenced in the main text) for phytoplankton cell counts. Epifluorescence stained cell volumes were converted to carbon biomass estimates using literature values. (b) These carbon estimates were converted here to chlorophyll estimates using a mean carbon-to-chlorophyll-*a* ratio of 47.2. The photoautotrophic taxonomic data were grouped into diatoms, picophytoplankton, and then all others (by difference of diatoms and picophytoplankton from the total photoautotrophic biomass). The resulting percentages of the total were sorted by total chlorophyll concentration and smoothed by a moving 10-point mean.

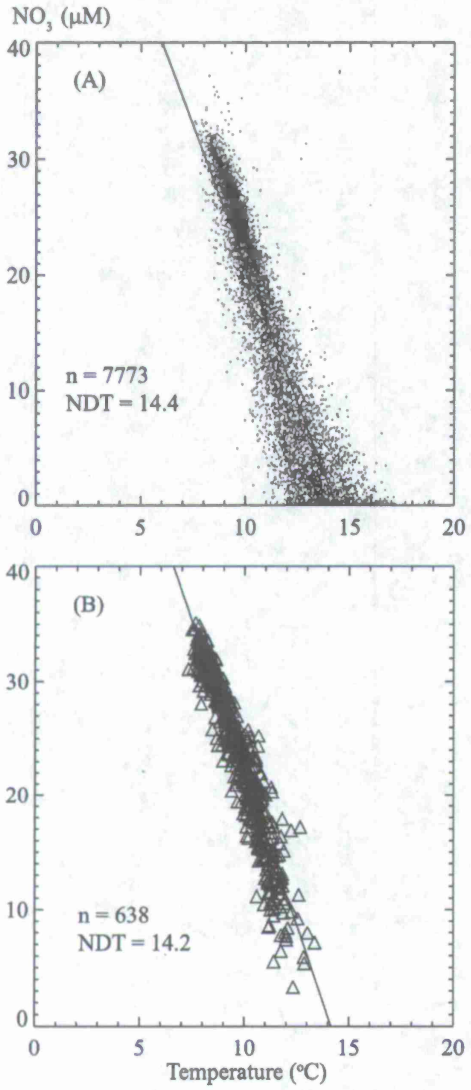

Figure 12. (a) Historical data linear regression for nitrate versus temperature measurements. Observations were restricted to the upper 200 m and latitude east of −123 W. (b) The same nitrate versus temperature regression for the BIODSACE 2008 field survey.

identified in this MB system. Some of this cell size trend may be due to pigment packaging: larger cells "package" pigments more densely thereby reducing the effective target area for photons to strike. It is also true that pigment packaging may have contributed to the reduction in the AFE_c values observed nearshore: the near-red chlorophyll-*a* absorption band overlaps with the fluorescence emission band and may contribute to fluorescence re-absorption within the cell [*Huot and Babin*, 2010].

[37] Nevertheless, two compelling pieces of evidence strongly suggest that this package effect may be secondary to a more broadly applicable taxonomic shift in σ_{PSII}. First, different values of σ_{PSII} for a mixed phytoplankton population tend to mix conservatively and may be predicted using simple mixing ratios based on the fluorescence properties of the predominant taxa [*Suggett et al.*, 2004]. This property of fluorescence properties in mixed phytoplankton populations may explain the "quasi-conservative" mixing of AFEc evident when plotted as a function of surface salinity (Figure 6), i.e., it is simply a consequence of the mixing of pelagic nanoflagellates (high AFEc, low I'k, and potentially large σ_{PSII}) with large coastal diatoms (low AFEc, high I'k, and potentially smaller σ_{PSII}). Second and as alluded to previously, prevailing depletion of essential micronutrients may place selective evolutionary pressure toward larger σ_{PSII} in pelagic species. It is far less iron-intensive to focus light harvesting capability upon expansion of antenna pigment complexes (requiring nitrogen) than it is to replicate additional photosynthetic reaction centers given their comparatively expensive iron requirements [*Strzepek and Harrison*, 2004]. Given that the source-water region for the California Current is one of the major High Nutrient Low Chlorophyll (HNLC) zones in the world ocean [*Martin et al.*, 1989], it would not be surprising that the flora endemic to these surface waters should exhibit a comparatively iron-conserving photosynthetic architecture.

5. Conclusions

[38] Consistent with the goal of the BIOSPACE program, this analysis indicates that the fundamental bio-optical and ecological distinction between coastal MB and California Current surface waters is the transition from microphytoplankton eutrophy to nanoflagellate mesotrophy. A coupled ecosystem-hydrodynamic model of the region would need to resolve this transition in a way that maintains fidelity to the observed physical and bio-optical property features of specific water masses. This analysis also suggests that there exists a very clear photophysiological distinction between these respective phytoplankton communities that

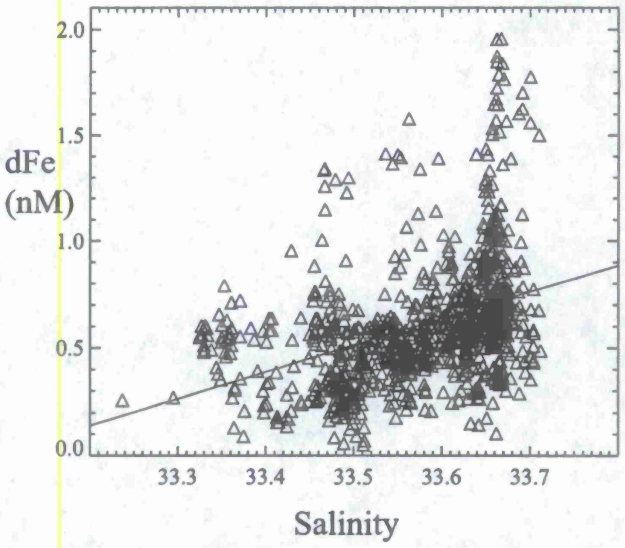

Figure 13. Surface dissolved iron data versus ship underway surface salinity measurements (*R/V New Horizon*) obtained during the MUSE experiment in the Monterey Bay region (19–31 August 2000).

may be expressed as a marked difference in irradiance saturation values and potentially the effective absorption cross-section of PSII. Circumstantial evidence from literature and historical data indicate that prevailing micronutrient conditions may be a contributing factor to this distinction; further studies involving collocated in situ variable fluorescence measurements (FRRF) and dissolved iron measurements are required to determine these relationships more conclusively.

Appendix A

A1. Calculation of In-Water Downwelling Irradiance

[39] The calculation of downwelling planar irradiance ($E_d(\lambda)$) at 1 nm spectral intervals was performed for each profile and each depth increment via an iterative hyperspectral attenuation scheme. Incident PAR was taken from the nearest space/time ship recording of surface PAR via the *R/V Point Sur* Underway Data Acquisition System (UDAS); specifically, the Biospherical QSR 2200 SPAR sensor. This is a broadband sensor and so the spectral decomposition over the 400–700 nm range was accomplished via application of a spectral atmospheric irradiance transmission model [*Gregg and Carder*, 1990]. Hyperspectral percentages of the total PAR output were applied to the QSR 2200 data for a full spectral decomposition estimate for the incident irradiance values. The scalar QSR 2200 irradiance data were converted to downelling planar irradiance by a constant factor of 0.8 [*Beardsley and Zaneveld*, 1969; *Jerlov*, 1976]. This was an approximation and the ratio E_d/E_o varies spectrally and as a function of the angular distribution of the light field. Broadband air/sea boundary reflectance was held constant at 4%.

[40] Hyperspectral downwelling planar irradiance ($E_d(\lambda, z)$) was then attenuated iteratively through the water column at (z) depths following the single scattering approximation [*Sathyendranath and Platt*, 1989] for the diffuse attenuation at each depth and wave band

$$K_d(\lambda, z) = \frac{a(\lambda, z) + bb(\lambda, z)}{\mu_d(\lambda)}. \quad \text{(A1)}$$

The spectral range for the mean cosine of downwelling irradiance ($\mu_d(\lambda)$) was estimated from published tabular values [*Morel and Maritorena*, 2001], and confined to a range of 0.767–0.901. Total absorption coefficients from the AC-9 instrument at 8 channels [412, 440, 488, 510, 532, 555, 650, 676 nm] and spectral backscattering coefficients at 3 channels [470, 532, 660 nm] from the ECO-BB3 sensor were used to interpolate hyperspectral diffuse attenuation values at 1 nm increments. Attenuation through the water column of a spectrally decomposed diffuse light field may be approximated by the Beer-Lambert Law

$$E_d(\lambda, z) = E_d(\lambda, z\text{-}1)e^{(-K_d(\lambda,z)\Delta z)}. \quad \text{(A2)}$$

[41] Iterative application of A2 was used to attenuate each wave band (1 nm) through the water column. Irradiance at each depth was then calculated as the sum of the spectrally decomposed irradiance over the PAR spectral range (400–700 nm).

A2. MUSE Dissolved Iron Data and MBARI Mooring Data

[42] Data on surface dissolvable iron were obtained from the MOOS Upper-Water column Science Experiment (MUSE) (19–31 August 2000) web site (http://www.mbari.org/MUSE/). Surface dissolvable iron determinations were converted to dissolved iron following methods described in *Johnson et al.* [2001]. The processed dissolved iron data were matched by time and location to the underway CTD data (UCTD data) obtained from a Seabird SBE-21 (SN 2960) Conductivity Temperature sensor mounted on the *R/V New Horizon*. The resulting matchup between dissolved iron determinations and underway salinities are plotted in Figure 13. Spatial maps of the dissolved iron distribution are available at the MBARI MUSE web site. Historical and recent temperature and salinity data from MBARI permanent moorings are also available from the MBARI web site (www.mbari.org/oasis/).

[43] **Acknowledgments.** This work is supported by the Naval Research Laboratory (NRL) project "Resolving Bio-Optical Feedbacks to Ocean/Atmosphere Dynamics," program element 0602435N and the NRL "Bio-Optical Studies of Predictability and Assimilation for the Coastal Environment" (BIOSPACE) program performed in collaboration with the Monterey Bay Aquarium Research Institute (MBARI). The authors thank Robert Helber, Andrew Quaid, Wesley Goode, Reiko Michisaki, Stephanie Anderson, Igor Shulman, Mark Hulbert, Marguerite Blum, and the crew of the *R/V Point Sur*. The authors also thank two anonymous reviewers and Grace Chang for helpful comments that improved the original manuscript.

References

Alpine, A. E., and J. E. Cloern (1985), Differences in *in vivo* fluorescence yield between three phytoplankton size classes, *J. Plankton Res.*, *7*, 381–390, doi:10.1093/plankt/7.3.381.

Babin, M., D. Stramski, G. M. Ferrari, H. Claustre, A. Bricaud, G. Obolensky, and N. Hoepffner (2003), Variations in the light absorption coefficients of phytoplankton, nonalgal particles, and dissolved organic matter in coastal waters around Europe, *J. Geophys. Res.*, *108*(C7), 3211, doi:10.1029/2001JC000882.

Beardsley, J. G. F., and J. R. V. Zaneveld (1969), Theoretical dependence of the near-asymptotic apparent optical properties on the inherent optical properties of sea water, *J. Opt. Soc. Am.*, *59*(4), 373–376, doi:10.1364/JOSA.59.000373.

Behrenfeld, M. J., K. Worthington, R. M. Sherrell, F. P. Chavez, P. Strutton, M. McPhaden, and D. M. Shea (2006), Controls on tropical Pacific Ocean productivity revealed through nutrient stress diagnostics, *Nature*, *442*(7106), 1025–1028, doi:10.1038/nature05083.

Beutler, M., K. H. Wiltshire, M. Arp, J. Kruse, C. Reineke, C. Moldaenke, and U. P. Hansen (2003), A reduced model of the fluorescence from the cyanobacterial photosynthetic apparatus designed for the in situ detection of cyanobacteria, *Biochim. et Biophys. Acta, Bioenerg.*, *1604*(1), 33–46, doi:10.1016/S0005-2728(03)00022-7.

Boyd, P. W., et al. (2004), The decline and fate of an iron-induced subarctic phytoplankton bloom, *Nature*, *428*(6982), 549–553, doi:10.1038/nature02437.

Breaker, L., and W. Broenkow (1994), The circulation in Monterey Bay and related processes, *Oceanogr. Mar. Biol.*, *32*, 1–64.

Bricaud, A., M. Babin, A. Morel, and H. Claustre (1995), Variability in the chlorophyll-specific absorption coefficients of natural phytoplankton: Analysis and parameterization, *J. Geophys. Res.*, *100*, 13,321–13,332, doi:10.1029/95JC00463.

Bricaud, A., H. Claustre, J. Ras, and K. Oubelkheir (2004), Natural variability of phytoplankton absorption in oceanic waters: Influence of the size structure of algal populations, *J. Geophys. Res.*, *109*, C11010, doi:10.1029/2004JC002419.

Bruland, K. W., E. L. Rue, and G. J. Smith (2001), Iron and macronutrients in California coastal upwelling regimes: Implications for diatom blooms, *Limnol. Oceanogr.*, *46*(7), 1661–1674, doi:10.4319/lo.2001.46.7.1661.

Chan, A. T. (1978), Comparative physiological study of marine diatoms and dinoflagellates in relation to irradiance and cell size. Part I. Growth under continuous light, *J. Phycol.*, *14*, 396–402, doi:10.1111/j.1529-8817.1978.tb02458.x.

Chavez, F. P., R. T. Barber, A. Huyer, P. M. Kosro, S. R. Ramp, T. Stanton, and B. Rojas de Mendoila (1991), Horizontal advection and the distribution

of nutrients in the coastal transition zone off northern California: Effects on primary production, phytoplankton biomass and species composition, *J. Geophys. Res.*, *96*, 14,833–14,848, doi:10.1029/91JC01163.

Chavez, F. P., J. T. Pennington, C. G. Castro, J. P. Ryan, R. P. Michisaki, B. Schlining, P. Walz, K. Buck, A. McPhayden, and C. A. Collins (2002), Biological and chemical consequences of the 1997–1998 El Niño in central California waters, *Prog. Oceanogr.*, *54*, 205–232, doi:10.1016/S0079-6611(02)00050-2.

Checkley, D. M., Jr., and J. A. Barth (2009), Patterns and processes in the California Current System, *Prog. Oceanogr.*, *83*, 49–64, doi:10.1016/j.pocean.2009.07.028.

Chelton, D. B., A. W. Bratkovich, R. L. Bernstein, and P. M. Kosro (1988), Poleward flow off central California during the spring and summer of 1981 and 1984, *J. Geophys. Res.*, *93*, 10,604–10,620, doi:10.1029/JC093iC09p10604.

Collins, C. A., J. T. Pennington, C. G. Castro, T. A. Rago, and F. P. Chavez (2003), The California Current System off Monterey, California: Physical and biological coupling, *Deep Sea Res., Part II*, *50*, 2389–2404, doi:10.1016/S0967-0645(03)00134-6.

Cullen, J. J. (1982), The deep chlorophyll maximum: Comparing vertical profiles of chlorophyll *a*, *Can. J. Fish. Aquat. Sci.*, *39*, 791–803, doi:10.1139/f82-108.

Cullen, J. J. (2008), Interactive comment on "Seaglider observations of variability in daytime fluorescence quenching of chlorophyll-a in Northeast Pacific coastal waters" by B. S. Sackman et al., *Biogeosci. Discuss.*, *5*, S1481–S1491.

Fager, E., and J. McGowan (1963), Zooplankton species groups in the North Pacific, *Science*, *140*, 453–460, doi:10.1126/science.140.3566.453.

Falkowski, P., and Z. S. Kolber (1995), Variations in chlorophyll fluorescence yields in phytoplankton in the world ocean, *Aust. J. Plant Physiol.*, *22*, 341–355, doi:10.1071/PP9950341.

Falkowski, P. G., and M. J. Oliver (2007), Mix and match: How climate selects phytoplankton, *Nat. Rev. Microbiol.*, *5*, 813–819, doi:10.1038/nrmicro1751.

Falkowski, P. G., R. M. Greene, and R. J. Geider (1992), Physiological limitations on phytoplankton productivity in the ocean, *Oceanography*, *5*(2), 84–91.

Fitzwater, S. E., K. S. Johnson, V. A. Elrod, J. P. Ryan, L. J. Coletti, S. J. Tanner, R. M. Gordon, and F. P. Chavez (2003), Iron, nutrient and phytoplankton biomass relationships in upwelled waters of the California coastal system, *Cont. Shelf Res.*, *23*(16), 1523–1544, doi:10.1016/j.csr.2003.08.004.

Flament, P. (2002), A state variable for characterizing water masses and their diffusive stability, *Prog. Oceanogr.*, *54*, 493–501, doi:10.1016/S0079-6611(02)00065-4.

Fofonoff, N. P. (1985), Physical properties of seawater: A new salinity scale and equation of state for seawater, *J. Geophys. Res.*, *90*, 3332–3342, doi:10.1029/JC090iC02p03332.

Freeland, H. J., G. Gatien, A. Huyer, and R. L. Smith (2003), Cold halocline in the northern California Current: An invasion of subarctic water, *Geophys. Res. Lett.*, *30*(3), 1141, doi:10.1029/2002GL016663.

Fujiki, T., K. Matsumoto, M. C. Honda, H. Kawakami, and S. Watanabe (2009), Phytoplankton composition in the subarctic North Pacific during autumn 2005, *J. Plankton Res.*, *32*(2), 179–191.

Gilstad, M., and E. Sakshaug (1990), Growth rates of ten diatom species from the Barents Sea at different irradiances and day lengths, *Mar. Ecol. Prog. Ser.*, *64*, 169–173, doi:10.3354/meps064169.

Gould, R. W., R. A. Arnone, and P. M. Martinolich (1999), Spectral dependence of the scattering coefficient in case 1 and case 2 waters, *Appl. Opt.*, *38*(12), 2377–2383, doi:10.1364/AO.38.002377.

Gregg, W. W., and K. L. Carder (1990), A simple spectral solar irradiance model for cloudless maritime atmospheres, *Limnol. Oceanogr.*, *35*(8), 1657–1675, doi:10.4319/lo.1990.35.8.1657.

Hooker, S. B., et al. (2005), Second SeaWiFS HPLC analysis round robin experiment (SeaHARRE-2), *NASA Tech. Memo. 212785*, NASA Goddard Space Flight Cent., Greenbelt, Md.

Hou, J.-J., B.-Q. Hunag, Z.-R. Cao, J.-X. Chen, and H.-S. Hong (2007), Effects of nutrient limitation on pigments in *Thalassiosira weissflogii* and *Prorocenturm donghaiense*, *J. Integr. Plant Biol.*, *49*(5), 686–697, doi:10.1111/j.1744-7909.2007.00449.x.

Huot, Y., and M. Babin (2010), Overview of fluorescence protocols: Theory, basic concepts, and practice, in *Chlorophyll a Fluorescence in Aquatic Sciences: Methods and Applications*, *Developments in Applied Phycology Ser.*, vol. 4, edited by D. J. Suggett, O. Prášil, and M. A. Borowitzka, pp. 31–74, Springer, New York, doi:10.1007/978-90-481-9268-7_3.

Jassby, A. D., and T. Platt (1976), Mathematical formulation of the relationship between photosynthesis and light for phytoplankton, *Limnol. Oceanogr.*, *21*(4), 540–547, doi:10.4319/lo.1976.21.4.0540.

Jeffrey, S. W., and M. Vesk (1997), Introduction to marine phytoplankton and their pigment signatures, in *Phytoplankton Pigments in Oceanography*, edited by S. W. Jeffrey, R. F. C. Mantoura, and S. W. Wright, pp. 37–84, U.N. Educ. Sci. and Cult. Organ., Paris.

Jerlov, N. G. (1976), *Marine Optics*, 231 pp., Elsevier Sci., Amsterdam.

Johnson, G., B. B. Prezelin, and R. V. M. Jovine (1997), Fluorescence excitation spectra and light utilization in two red tide dinoflagellates, *Limnol. Oceanogr.*, *42*, 1166–1177, doi:10.4319/lo.1997.42.5_part_2.1166.

Johnson, K. S., F. P. Chavez, and G. E. Friederich (1999), Continental-shelf sediment as a primary source of iron for coastal phytoplankton, *Nature*, *398*(6729), 697–700, doi:10.1038/19511.

Johnson, K. S., F. P. Chavez, V. A. Elrod, S. E. Fitzwater, J. T. Pennington, K. R. Buck, and P. M. Waltz (2001), The annual cycle of iron and the biological response in central California coastal waters, *Geophys. Res. Lett.*, *28*, 1247–1250, doi:10.1029/2000GL012433.

Jolliff, J. K., J. C. Kindle, I. Shulman, B. Penta, M. A. M. Friedrichs, R. Helber, and R. A. Arnone (2009), Summary diagrams for coupled hydrodynamic-ecosystem model skill assessment, *J. Mar. Syst.*, *76*(1-2), 64–82, doi:10.1016/j.jmarsys.2008.05.014.

Kamykowski, D., S. J. Zentara, J. M. Morrison, and A. C. Switzer (2002), Dynamic global patterns of nitrate, phosphate, silicate, and iron availability and phytoplankton community composition from remote sensing data, *Global Biogeochem. Cycles*, *16*(4), 1077, doi:10.1029/2001GB001640.

Kiefer, D. A. (1973), Fluorescence properties of natural phytoplankton, *Mar. Biol.*, *22*, 263–269, doi:10.1007/BF00389180.

Kiefer, D. A., and R. A. Reynolds (1992), Advances in understanding phytoplankton fluorescence and photosynthesis, in *Primary Productivity and Biogeochemical Cycles in the Sea*, edited by P. Falkowski and A. D. Woodhead, pp. 155–174, Plenum Press, New York.

King, A. L., and K. A. Barbeau (2011), Dissolved iron and macronutrient distributions in the southern California Current System, *J. Geophys. Res.*, *116*, C03018, doi:10.1029/2010JC006324.

Kolber, Z., and P. G. Falkowski (1993), Use of active fluorescence to estimate phytoplankton photosynthesis in situ, *Limnol. Oceanogr.*, *38*(8), 1646–1665, doi:10.4319/lo.1993.38.8.1646.

Krause, G. H., and E. Weis (1991), Chlorophyll fluorescence and photosynthesis: The basics, *Annu. Rev. Plant Physiol. Plant Mol. Biol.*, *42*, 313–349, doi:10.1146/annurev.pp.42.060191.001525.

Lee, Z.-P., C. Hu, D. Gray, B. Casey, R. A. Arnone, A. Weidemann, R. Ray, and W. Goode (2007), Properties of coastal waters around the U.S.: Preliminary results using MERIS data, paper presented at Envisat Symposium 2007, Eur. Space Agency, Montreaux, Switzerland, 23–27 Apr.

Li, W. K. W. (2002), Macroecological patterns of phytoplankton in the northwestern North Atlantic Ocean, *Nature*, *419*, 154–157, doi:10.1038/nature00994.

Loftus, M., and H. Seliger (1975), Some limitations of the in vivo fluorescence technique, *Chesapeake Sci.*, *16*(2), 79–92, doi:10.2307/1350685.

Lorenzen, C. J. (1966), A method for the continuous measurement of *in vivo* chlorophyll concentration, *Deep Sea Res. Oceanogr. Abstr.*, *13*(2), 223–227, doi:10.1016/0011-7471(66)91102-8.

Lynn, R. J. (1986), The subarctic and northern subtropical fronts in the eastern North Pacific Ocean in spring, *J. Phys. Oceanogr.*, *16*(2), 209–222, doi:10.1175/1520-0485(1986)016<0209:TSANSF>2.0.CO;2.

Martin, J. H., R. M. Gordon, S. Fitzwater, and W. W. Broenkow (1989), Vertex: Phytoplankton/iron studies in the Gulf of Alaska, *Deep Sea Res., Part A*, *36*(5), 649–680, doi:10.1016/0198-0149(89)90144-1.

Mauzerall, D., and N. L. Greenbaum (1989), The absolute size of a photosynthetic unit, *Biochim. Biophys. Acta*, *974*, 119–140, doi:10.1016/S0005-2728(89)80365-2.

Maxwell, K., and G. N. Johnson (2000), Chlorophyll fluorescence—A practical guide, *J. Exp. Bot.*, *51*(345), 659–668, doi:10.1093/jexbot/51.345.659.

Miller, C. B., B. W. Frost, B. Booth, P. A. Wheeler, M. R. Landry, and N. Welschmeyer (1991), Ecological processes in the subarctic Pacific: Iron limitation cannot be the whole story, *Oceanography*, *4*, 71–78.

Mitchell, B. G., et al. (2000), Determination of spectral absorption coefficients of particles, dissolved material and phytoplankton for discrete water samples, in *Ocean Optics Protocols For Satellite Ocean Color Sensor Validation, Revision 2*, edited by G. S. Fargion, J. L. Mueller, and C. R. McClain, pp. 125–153, NASA Goddard Space Flight Cent., Greenbelt, Md.

Moore, C. M., D. J. Suggett, A. E. Hickman, Y.-N. Kim, J. F. Tweddle, J. Sharples, R. J. Geider, and P. M. Holligan (2006), Phytoplankton photoacclimation and photoadaptation in response to environmental gradients in the sea, *Limnol. Oceanogr.*, *51*(2), 936–949, doi:10.4319/lo.2006.51.2.0936.

Morel, A., and S. Maritorena (2001), Bio-optical properties of oceanic waters: A reappraisal, *J. Geophys. Res.*, *106*(C4), 7163–7180, doi:10.1029/2000JC000319.

Osborn, D. A., M. W. Silver, C. G. Castro, S. M. Bros, and F. P. Chavez (2007), The habitat of mesopelagic scyphomedusae in Monterey Bay, California, *Deep Sea Res., Part I*, *54*(8), 1241–1255, doi:10.1016/j.dsr.2007.04.015.

Paduan, J. D., and L. K. Rosenfeld (1996), Remotely sensed surface currents in Monterey Bay from shore-based HF radar (Coastal Ocean Dynamics Application Radar), *J. Geophys. Res.*, *101*, 20,669–20,686, doi:10.1029/96JC01663.

Pegau, W. S., D. Gray, and J. R. V. Zaneveld (1997), Absorption of visible and near-infrared light in water: The dependence on temperature and salinity, *Appl. Opt.*, *36*(24), 6035–6046, doi:10.1364/AO.36.006035.

Pennington, J. T., and F. P. Chavez (2000), Seasonal fluctuations of temperature, salinity, nitrate, chlorophyll and primary production at station H3/M1 over 1989–1996 in Monterey Bay, California, *Deep Sea Res. Part II*, *47*, 947–973, doi:10.1016/S0967-0645(99)00132-0.

Pope, R. M., and E. S. Fry (1997), Absorption spectrum (380–700 nm) of pure water: Part II. Integrating cavity measurements, *Appl. Opt.*, *36*(33), 8710–8723, doi:10.1364/AO.36.008710.

Ramp, S. R., et al. (2009), Preparing to predict: The Second Autonomous Ocean Sampling Network (AOSN-II) experiment in the Monterey Bay, *Deep Sea Res., Part II*, *56*(3-5), 68–86, doi:10.1016/j.dsr2.2008.08.013.

Redfield, A. C., B. H. Ketchum, and F. A. Richards (1963), The influence of organisms on the compostition of seawater, in *The Sea*, vol. 2, edited by M. N. Hill, pp. 26–77, Wiley Interscience, New York.

Riegman, R., and G. W. Kraay (2001), Phytoplankton community structure derived from HPLC analysis of pigments in the Faroe-Shetland Channel during summer 1999: The distribution of taxonomic groups in relation to physical/chemical conditions in the photic zone, *J. Plankton Res.*, *23*, 191–205, doi:10.1093/plankt/23.2.191.

Rines, J. E. B., M. N. McFarland, P. L. Donaghay, and J. M. Sullivan (2010), Thin layers and species-specific characterization of the phytoplankton community in Monterey Bay, California, USA, *Cont. Shelf Res.*, *30*, 66–80, doi:10.1016/j.csr.2009.11.001.

Roden, G. I. (1991), Subarctic-subtropical transition zone of the North Pacific: Large-scale aspects and mesoscale structure, in *Biology, Oceanography, and Fisheries of the North Pacific Transition Zone and Subarctic Frontal Zone*, *NOAA Tech. Rep. NMFS 105*, edited by J. A. Wetherall, pp. 1–38, Natl. Mar. Fish. Serv., NOAA, Silver Spring, Md.

Ryan, J. P., F. P. Chavez, and J. G. Bellingham (2005), Physical-biological coupling in Monterey Bay, California: Topographic influences on phytoplankton ecology, *Mar. Ecol. Prog. Ser.*, *287*, 23–32, doi:10.3354/meps287023.

Ryan, J. P., A. M. Fischer, R. M. Kudela, J. F. R. Gower, S. A. King, R. Marin Iii, and F. P. Chavez (2009), Influences of upwelling and downwelling winds on red tide bloom dynamics in Monterey Bay, California, *Cont. Shelf Res.*, *29*(5-6), 785–795, doi:10.1016/j.csr.2008.11.006.

Sackmann, B. S., M. J. Perry, and C. C. Eriksen (2008), Seaglider observations of variability in daytime fluorescence quenching of chlorophyll-*a* in Northeastern Pacific coastal waters, *Biogeosci. Discuss.*, *5*(4), 2839–2865, doi:10.5194/bgd-5-2839-2008.

Sathyendranath, S., and T. Platt (1989), Computation of aquatic primary production: Extended formalism to include effect of angular and spectral distribution of light, *Limnol. Oceanogr.*, *34*(1), 188–198, doi:10.4319/lo.1989.34.1.0188.

Stegmann, P. M., M. R. Lewis, C. O. Davis, and J. J. Cullen (1992), Primary production estimates from recordings of solar-stimulated fluorescence in the equatorial Pacific at 150°W, *J. Geophys. Res.*, *97*(C1), 627–638, doi:10.1029/91JC02014.

Storlazzi, C. D., M. A. McManus, and J. D. Figurski (2003), Long-term, high-frequency current and temperature measurements along central California: Insights into upwelling/relaxation and internal waves on the inner shelf, *Cont. Shelf Res.*, *23*, 901–918, doi:10.1016/S0278-4343(03)00045-1.

Stow, C. A., J. Jolliff, D. J. McGillicuddy Jr., S. C. Doney, J. I. Allen, M. A. M. Friedrichs, K. A. Rose, and P. Wallhead (2009), Skill assessment for coupled biological/physical models of marine systems, *J. Mar. Syst.*, *76*(1-2), 4–15, doi:10.1016/j.jmarsys.2008.03.011.

Strickland, J. D. H. (1968), Continuous measurement of *in vivo* chlorophyll; a precautionary note, *Deep Sea Res. Oceanogr. Abstr.*, *15*(2), 225–227, doi:10.1016/0011-7471(68)90043-0.

Strzepek, R. F., and P. J. Harrison (2004), Photosynthetic architecture differs in coastal and oceanic diatoms, *Nature*, *431*(7009), 689–692, doi:10.1038/nature02954.

Suggett, D. J., H. L. MacIntyre, and R. J. Geider (2004), Evalutation of biophysical and optical determinations of light absorption by photosystem II in phytoplankton, *Limnol. Oceanogr. Methods*, *2*, 316–332, doi:10.4319/lom.2004.2.316.

Suggett, D. J., C. M. Moore, A. E. Hickman, and R. J. Geider (2009), Interpretation of fast repetition rate (FRR) fluorescence: Signatures of phytoplankton community structure versus physiological state, *Mar. Ecol. Prog. Ser.*, *376*, 1–19, doi:10.3354/meps07830.

Takeda, S. (2011), Iron and phytoplankton growth in the subarctic North Pacific, *Aqua-BioSci. Monogr.*, *4*(2), 41–93, doi:10.5047/absm.2011.00402.0041.

Tully, J. P., and F. G. Barber (1960), An estuarine analogy in the subarctic Pacific Ocean, *J. Fish. Res. Board Can.*, *17*, 91–112, doi:10.1139/f60-007.

Walsh, J. J. (1988), *On the Nature of Continental Shelves*, 520 pp., Academic, San Diego, Calif.

Warn-Varnas, A. (2007), Water masses in the Monterey Bay during summer of 2000, *Cont. Shelf Res.*, *27*(10-11), 1379–1398, doi:10.1016/j.csr.2007.01.004.

Wilkerson, F. P., R. C. Dugdale, R. M. Kudela, and F. P. Chavez (2000), Biomass and productivity in Monterey Bay, California: Contribution of the large phytoplankton, *Deep Sea Res., Part II*, *47*(5-6), 1003–1022, doi:10.1016/S0967-0645(99)00134-4.

Yu, X., T. Dickey, J. Bellingham, D. Manov, and K. Streitlien (2002), The application of autonomous underwater vehicles for interdisciplinary measurements in Massachusetts and Cape Cod Bays, *Cont. Shelf Res.*, *22*, 2225–2245, doi:10.1016/S0278-4343(02)00070-5.

Zaneveld, J. R. V., J. C. Kitchen, and C. Moore (1994), The scattering error correction of reflecting-tube absorption meters, *Proc. SPIE*, *2258*, 44–55, doi:10.1117/12.190095.